Materials Research Innovations

ISSN: 1432-8917 (Print) 1433-075X (Online) Journal homepage: https://www.tandfonline.com/loi/ymri20

The perovskite structure—a review of its role in ceramic science and technology

A.S. Bhalla, Ruyan Guo & Rustum Roy

To cite this article: A.S. Bhalla, Ruyan Guo & Rustum Roy (2000) The perovskite structure—a review of its role in ceramic science and technology, Materials Research Innovations, 4:1, 3-26, DOI: 10.1007/s100190000062

To link to this article: https://doi.org/10.1007/s100190000062

Mat Res Innovat (2000) 4:3–26

REVIEW

A.S. Bhalla · Ruyan Guo · Rustum Roy

The perovskite structure – a review of its role in ceramic science and technology

Received: 29 November 1999 / Accepted: 3 July 2000

Abstract Starting with the history of the fundamental science of the relation of structure to composition delineated completely by Goldschmidt, we use the perovskite structure to illustrate the enormous power of crystal chemistry-based intelligent synthesis in creating new materials.

The perovskite structure is shown to be the single most versatile ceramic host. By appropriate changes in *composition* one can modify the most significant electroceramic dielectric ($BaTiO_3$ and its relatives) phase in industry, into metallic conductors, superconductors or the highest pressure phases in the earth. After an historical introduction of the science, detailed treatment of the applications is confined to the most recent research on novel uses in piezoelectric, ferroelectric and related applications.

Keywords Perovskite · Crystal-chemistry · Tolerance factor · Ferroics · Electro-ceramics

1 Introduction: Prewar history of the emergence of perovskite as the key ternary ceramic phase

1.1 The short list of important ceramic phases

Ceramics (processed inorganic materials) are by far the highest volume and highest tonnage materials made and used by humankind. Yet, there are only a half dozen specific ceramic *phases* that dominate human use of such materials not only in terms of volume, weight, etc., but also in terms of technological significance. Any list of such would contain at least the following:

– Quartz – which as sand is ubiquitous in rocks, beaches, soil, buildings, and roads.
– Mullite – the principal component both of crude and refined pottery of all kinds, or bricks, and of a great deal of high tech ceramics.
– Calcium silicates – "Ca_3SiO_5, Ca_2SiO_4 and $Ca_3Al_2O_6$" – and their hydration products, the key constituents of cement and concrete, which at 1500 million tons/year is humankind's largest tonnage manufactured product.
– "Al_2O_3" – the key unary oxide of ceramic technologies from hard grinding materials to all kinds of refractory ceramics, to laser hosts and gems (rubies and sapphires).
– "TiO_2" – the required high refractive index material in a variety of high volume (e.g., paint) uses and the key ingredient in electroceramics.

Each of these phases – defined by *both* crystal *structure* and *composition* – is useful because it has one or two special properties and applications. Well may one ask: Are there ternary structures that are multifunctional, that is, that can serve as the appropriate crystallographic host for a wide variety of useful properties and functions? Examination of lists of the main ternary crystal structures [1] reveals that among thousands of complex structures there are only a dozen or so structures which dominate the entire world of useful ceramics. Among these the A_2BX_4 structure, spinel; and the ABX_3 structure, perovskite, stand out by a wide margin, and perovskite is far ahead of spinel as the single structure which, with skilled chemical manipulation, can produce an incredibly wide array of phases with totally different functions (Fig. 1).

1.2 Perovskite proves the error of the tructure-property cliché of early materials scientists

The emphasis on the importance of the "structure-property" relation as the key to the understanding of "materials science" was a curious half-truth of the 1950s mistakenly imposed on generations of students. In trying to emphasize the

A.S. Bhalla (✉) · R. Guo · R. Roy
Materials Research Laboratory,
The Pennsylvania State University,
University Park, PA 16802, USA
e-mail: asb2@psu.edu
Tel.: +1-814-8659232, Fax: +1-814-8637846

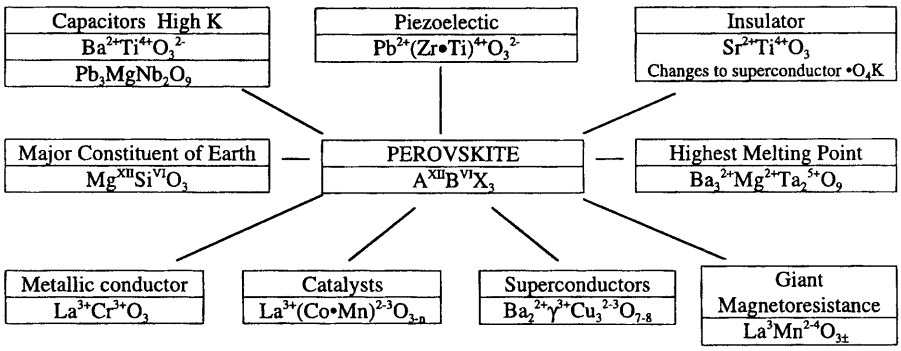

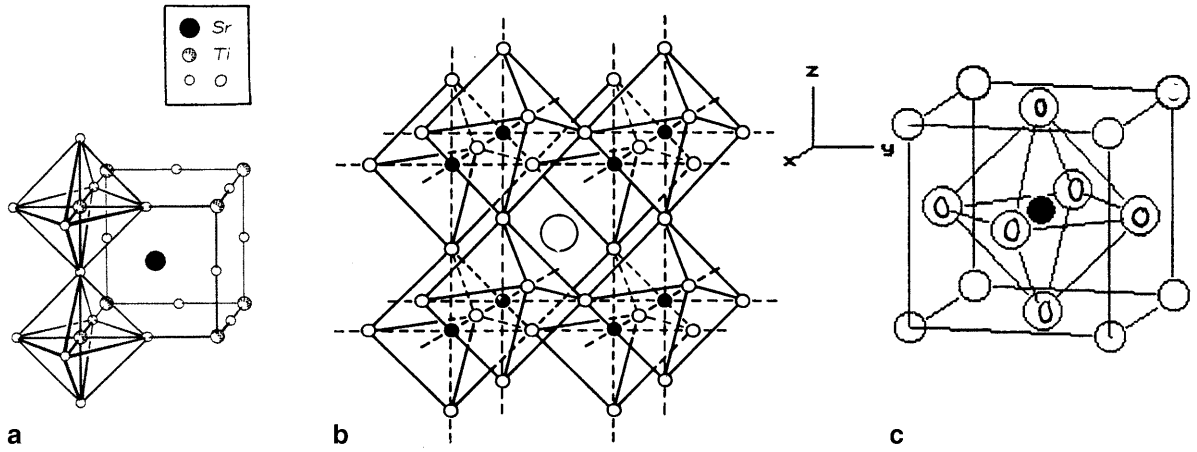

Fig. 1 Perovskite – the maximum multifunctional structure

Fig. 2 (**a**) The [ideal perovskite] structure, illustrated for $SrTiO_3$ [2–4]. Note the corner-shared octahedra extending in three dimensions. (**b**) and (**c**) Some other ways of presenting perovskite structure

importance of crystal or atomic structure or microstructure as opposed merely to gross composition, this facile expression led to the opposite error that structure was *the* necessary (but by implication also sufficient) predictor of properties. That is, of course, manifestly absurd. The perovskite structure stands as the outstanding example proving the error of this over-simplistic cliché.

1.3 Mineral discovery

Perovskite is the name for a structural family, in addition to being the name for a particular mineral with the composition, $CaTiO_3$. This confusion between the structural name, and a compositional entity is overweening in materials science, but very rarely dealt with explicitly. In Muller and Roy's textbook [1] this nomenclature issue is dealt with extensively, and a formalism developed that when used as a structural descriptor (see [1] p 8 for detailed treatment of nomenclature) the original mineral composition would be enclosed in square brackets. Thus $[CaTiO_3]$ stands for the perovskite structures not the composition $CaTiO_3$. This formalism has not been widely adopted and confusion continues.

1.4 The structure

The [ideal perovskite] has a very simple arrangement of ions that is illustrated in Fig. 2. The cubic (isometric) structure is typified not by $CaTiO_3$ but by $SrTiO_3$ with a=3.905 Å, Z=1, and space group O_h^1–Pm3m. The Ti atoms are located at the corners, and the Sr atoms at the center of the cube. The oxygen is placed at the centers of the twelve cube edges, giving corner-shared strings of TiO_6 octahedra, which extend infinitely in three dimensions. The TiO_6 octahedra are perfect with 90 ° angles and six equal Ti-O bonds at 1.952 Å. Each Sr atom is surrounded by twelve equidistant oxygen at 2.761 Å. The structural formula written explicitly with coordination number of each ion and local symmetry (see Muller and Roy) is as follows:

$$Sr^{XII}Ti^{VI}O_3^{VI}\left\{Sr^{XII}_{[m3m]}Ti^{VI}_{[m3m]}O^{(II)+IV}_{3[4/mm]}\right\} \quad (1)$$

The [ideal perovskite] can also be regarded as a cubic close-packed structure in which the oxygen and the Sr atoms are stacked in cubic close-packed layers along the cubic [111] direction. Some of the resulting octahedral holes are occupied by Ti atoms. Some other ways of presenting the structure are shown in Fig. 2(b) and 2(c).

1.5 Crystal chemistry begins

Historically however, perovskite would have remained a mineralogical curiosity were it not for V.M. Gold-

schmidt, the founder of the science of crystal chemistry, and his school of geochemists in Oslo. Goldschmidt made and studied a large number of the first synthetic perovskites with different compositions, including $BaTiO_3$, in 1924–26 [5]. This quotation is taken from Goldschmidt's classic, the single most important reference in the entire history of materials synthesis, entitled "Geochemische Verteilungsgesetze der Elemente":

In unserem Institut sind mehrere Reihen von Verbindungen ABX_3 untersucht worden, um die Morphotropie-Beziehungen dieser Stoffe festzustellen. Ich hoffe, bei späterer Gelegenheit ausführlicher auf diese Verbindungen zurückkommen zu können. An dieser Stelle seien die Struktur-Daten eines speziellen ABX_3-Typus nach unsern Messungen zusammengestellt, nämlich die Daten des Perowskit-Typus.

But not only did Goldschmidt synthesize a large number of such isostructural phases but he started what was to become the world's first school of *crystal* chemistry, by determining the crystal *structures* of each of the phases, of the ABX_3 *compositions*. This, in an era when powder x-ray diffraction was in its infancy.

A second quotation from this monograph records the fact that Goldschmidt himself made all the compounds and that he, Tom Barth and Willy Zachariasen each did some of the x-ray structures, and measured lattice parameters which prove to be amazingly accurate today.

Perowskit-Struktur:

Die Perowskit-Struktur wurde von T. Barth (in [5]) am Perowskit, $CaTiO_3$, am $NaNbO_3$, sowie am Dysanalyt (Mischcrystall $CaTiO_3$–$NaNbO_3$) studiert. Eine große Anzahl von Substanzen mit Perowskit-Struktur wurde 1925 and 1926 von mir dargestellt, und teils von mir selbst, teils von T. Barth, teils von W. Zachariasen untersucht; die meisten dieser Stoffe sind bereits in 6. Erwähnt.

Goldschmidt then went on to establish what remains after seventy-five years the first (and lasting) principles of materials synthesis:

- The radius of the ions is fundamental (his table of radii was the first) to structure.
- The radius ratio Rc/Ra determines the coordination number of the cation (= the polyhedron formed.)
- The packing of polyhedra follows simple rules (later codified by Pauling [6]).

That the perovskite structure was central to the birth of these ideas may be found in the next paragraph where Goldschmidt introduces the concept of the "tolerance factor" (T.F.) for the perovskite arrangement of interpenetrating dodecahedra and octahedra, i.e., how far from ideal packing can the ionic sizes move and still be "tolerated" by the perovskite structure?

Ich fand dabei die Entstehung der Perowskit-struktur an bestimmte numerische Beziehungen zwischen den Radien der Krystallbausteine geknüpft ist. Für unsere Betrachtungen hier ist wesntlich db der Toleranzfaktor

Table 1 Bestimmungen der Gitterdimensionen liegen an folgenden Crystallen dieser Art Vor:

Verbindung	a	Literature (no. referring to that of in [5])
$CaTiO_3$[1]	3.80±0.02	6, 10
$SrTiO_3$	3.92±0.02	6
$BaTiO_3$	3.97±0.02	6
KIO_3	4.46±0.02	6
$RbIO_3$	4.52±0.02	6
$NaNbO_3$	3.98±0.02	10
$KNbO_3$	4.01±0.02	6
$CaZrO_3$	3.99±0.10	6

$$t = \frac{R_a + R_x}{\sqrt{2} \cdot (R_b + R_x)} \tag{2}$$

Bei Perowskitstrukturen einen Wert zwischen 0,8 and 1,00 besitzt.

It should be noted that the reason why Goldschmidt's (and Pauling's) crystal chemistry has been so successful in guiding the intelligent materials synthesis of literally thousands of new and many useful phases, is that their rules and laws are based on hundreds of empirical measurements which do not change. Thirty years before each III-V and II-VI semiconductor was "discovered," Goldschmidt had listed them *all* casually on one table in the same volume referred to above.

1.6 The first *useful* property in a perovskite ($BaTiO_3$) – dielectric constant

The next set of key events in the history of the emergence of the perovskite structure as the preeminent high-tech ceramic materials occurred during WWII, and the history is partly lost in wartime secrecy and lack of open publications.

Nevertheless, the history of $BaTiO_3$ is closely tied to a very different material-muscovite mica $KMg_3(AlSi_3)O_{10}(OH)_2$. Mica was the key insulator in most capacitors (with a κ of 10) and had to be imported by the Allies, Germany, Russia, and Japan mainly from India (and Brazil). Supply lines were tenuous. Demand was skyrocketing. A key wartime R/D goal for all those countries was to find a substitute dielectric (with a κ of 80 as the starting point). Our colleague W.R. Buessem, then the Director of Science Research in Siemens, Germany reported that by 1940–1941 various alkaline earth titanates were in production. Shot-down fighter planes became the source of this intelligence for the West. But whether from this source or directly from their own backgrounds, in Cleveland in The TAM labs, Wainer and Solomon had identified $BaTiO_3$ [7] as possibly having the highest κ.

In 1945 Wul and Goldman [8] in Moscow also found the same compound as being the most promising, and in Tokyo Ogawa [9] identified the same winner: $BaTiO_3$ (see history by Cross and Newnham [10]). The historians of science may find this to be an example of Rupert

Sheldrake's morphogenetic field [11] where the ideas are pregnant in the atmosphere worldwide, and crystallize out at the same time in different places. Or else one may simply see it as the result of systematic analysis of the same problem by different scientists all over the world. A final historic footnote is that one of the authors (R.R.) arrived in the US in 1945 with the objective of saving India's mica industry from the inroads of substitutes. By 1950 he was fully involved in the synthesis and crystal chemistry of the material, $BaTiO_3$ – which almost totally displaced mica!

1.7 The link to ferroelectricity

It was von Hippel and the MIT Laboratory for Insulation Research [12] which recognized the reason for the extraordinary values of 'κ' which were being found. In quick succession, Ginsburg, 1946 [13], Megaw, 1946 [14], and Blattner, Matthias and Merz, 1947 [15] in Europe confirmed the theory, re-did the structure, and grew a few single crystals to prove the point. By 1948 several authors [16–20] had studied the optical domain structure and improved on the phenomenology and the structure and change involved. Several major industry groups entered the field, notably Bell Telephone Labs. In 1950 two separate groups at Penn State entered the scene. Pepinsky and his large group in the Physics Department on ferroelectricity, which during the next four years included major figures in the field (Merz, Matthias, Megaw, Shirane, Jona, etc.) and Roy and Osborn in Geochemistry who embarked on the systematic synthesis and crystal chemistry and phase equilibria of complex oxides. Samples which were sent back and forth for measurement was the link between the groups.

1.8 Two perovskite "functions": ferroelectricity and superconductivity compared

To bracket and to conclude the history of the utility of perovskite we jump ahead forty years to the discovery of high T_C superconductivity. Whereas for years the Penn State group was literally the only one working on the synthesis and systematic crystal chemistry of the ferroelectrics, literally hundreds of groups jumped in within months of the discovery to study the superconductors.

Tables 2 and 3 make an interesting comparison to debate both the nature of advances in science and science policy, and especially investment in science. The actual advance in the key functions – dielectric constant in one case and transition temperature in the other was certainly greater in $BaTiO_3$ (a factor of 100) than in $YBa_2Cu_3O_{7-\delta}$ (factor of 3). The ratio of the speed and magnitude of the impact on technology was of course even more greatly in favor of $BaTiO_3$. Yet both the absolute amount and the rate of research effort put into the superconductor was in the opposite ratio, much, much higher. The pay-off so far at least has been vastly smaller for superconductors.

Table 2 Discoveries (past) – comparative research history and strategy

	Ferroelectricity TiO_2-$MgTiO_3$ $BaTiO_3$	Superconductivity $LaBaCuO_4$ $YBa_2Cu_3O_{7-\delta}$
Discovery	USA ~ Simultaneously: USA, USSR, Japan 1944–1946 κ=10	Switzerland-Japan ~ Simultaneously: Huntsville, Beijing, Bangalore 1986–1987 T_C=23K
Property advance	→100 →30,000	→36K →90K
Research effort for Proof of	100 p.y. to major payoff	(1000 p.y. and far to go to ??)

Table 3 Comparison, history and strategy – $BaTiO_3$:HTSC

	Ferroelectricity TiO_2-$MgTiO_3$ $BaTiO_3$	Superconductivity $LaBaCuO_4$ $YBa_2Cu_3O_{7-\delta}$
US Position	Industry in commanding position	Industry very weak. Universities very weak in relevant fields
Technological	Drop-in replacement	~ No products.
Prospects	into existing	Short-term prospects unclear
Technological	enormous	Major Impact *Improbable*
Reality	capacitor industry, Piezoelectrics, Pyroelectrics, Electrooptics	in 10–15 year frame

2 Synthesis, crystal chemistry, and phase diagrams

2.1 Synthesis

All the usual ceramic reaction methods are used for synthesizing the most used perovskite phases.

2.1.1 Solid state reaction

By far the most commonly used process is that of thoroughly mixing oxides (or carbonates and oxides) and firing at temperatures of >2/3 m.p. for periods up to ten hours. The process poses special problems for the cases where one oxide, especially a toxic one like Pb, may vaporize in part during the long reaction times.

2.1.2 Solution technologies – sol-gel and others

Starting in 1950 several perovskites phases were probably the first such nonsilicate ceramics ever made by the sol-gel techniques which had been developed by Roy at Penn State in 1948 [21]. Sol-gel methods were routinely applied to many of the aluminate, titanate, and complex mixed cation phases (see later) made by one of the authors (R.R.) and his students [22–25] by the mid 1950s.

In the last decade or two, sol-gel techniques have finally attracted wider attention especially for making thin films at low temperatures. In our own rather extensive work we have been able to grow many highly oriented perovskites such as $SrTiO_3$ on $SrTiO_3$ "single crystals" as low as 600 °C from thin gel layers spun on to the substrates. References [26–30] give examples of some of these synthesis and processing studies on various perovskites.

2.1.3 Hydrothermal

This method [31] was also used very early on to synthesize and check the thermodynamic stability of $BaTiO_3$ and many other perovskites in the fifties [32]. Recently there has been considerable activity in making $BaTiO_3$ at very low temperatures by this route [33–35].

2.1.4 Hydrothermal-electrochemical

Following the work of Hawkins and Roy [36] on using an electric field to lower hydrothermal synthesis temperature, Yoshimura et al. have demonstrated the ability to synthesize $BaTiO_3$ by using such an electric field in a hydrothermal bomb at temperatures between 100 and 200 °C [37].

2.1.5 Microwave synthesis

In a conventional furnace $BaCO_3$+TiO_2 reacts in a few hours at 1200 °C to form first Ba_2TiO_4 and then very slowly the assemblage react to give increasing amounts of $BaTiO_3$.

Table 4 Phase sequences and times of reaction in synthesis of $BaTiO_3$ (starting precursors: $BaCO_3$ and TiO_{2-x})

Conditions Temp/Time	Phases identified by XRD and relative peak intensities in %			
	$BaCO_3$	TiO_{2-x}	Ba_2TiO_4[a]	Tet.-$BaTiO_3$[b,c]
Conventional:				
900 °C/2 min	57	43	–	–
950 °C/2 min	67	33	–	–
950 °C/1 h	62	23	14	–
1100 °C/1 h	36	37	26	–
1200 °C/1 h	30	37	33	–
1300 °C/1 h	–	–	100	–
Microwave Method:				
250 °C/0 min	45	51	4	–
400 °C/0 min	25	22	48	5
500 °C/1 min	12	10	54	24
600 °C/5 min	11	13	29	47
700 °C/5 min	6	8	16	70
900 °C/5 min	–	1	–	99

[a] Compare 4% $BaTiO_3$ (hex.) 0 min (microwave)
[b] Compare 0% $BaTiO_3$ after 1 h (conventional)
[c] Compare 99% $BaTiO_3$ (tet.) 5 min (microwave)

In a 2.450 GHz microwave field we find the most remarkable differences, especially when we work in systems using slightly reduced titanates or tantalates, etc. [38]. Thus one can observe the formation of $BaTiO_3$ in *one to two minutes*, and also note completely new reaction paths. For example appearance of hexagonal $BaTiO_3$ (unheard of at these temperatures) and the fact that no Ba_2TiO_4 is ever formed. Data are shown in Table 4 on a very effective and likely to be commercialized process for most electroceramics. Because of its simplicity and speed, microwave sintering is especially attractive for Pb-containing perovskites, because it minimizes the Pb-loss.

2.1.6 PVD methods – laser ablation, MBE

As the movement towards integration of the capacitative function into silicon circuitry grows, all the well-developed thin film methods are, of course, routinely being applied to perovskites. Thin film ferroelectrics are a major field of research and references to two or three symposium proceedings and journals will show how extensive this work is [39–41].

2.2 Crystal chemistry

Just as Goldschmidt had pioneered in building the foundation of crystal chemistry on the basis of extensive synthesis, so also Roy and his students took the crystal chemistry of perovskites to the next level, especially involving *multiple ion* substitution on the same site – a ba-

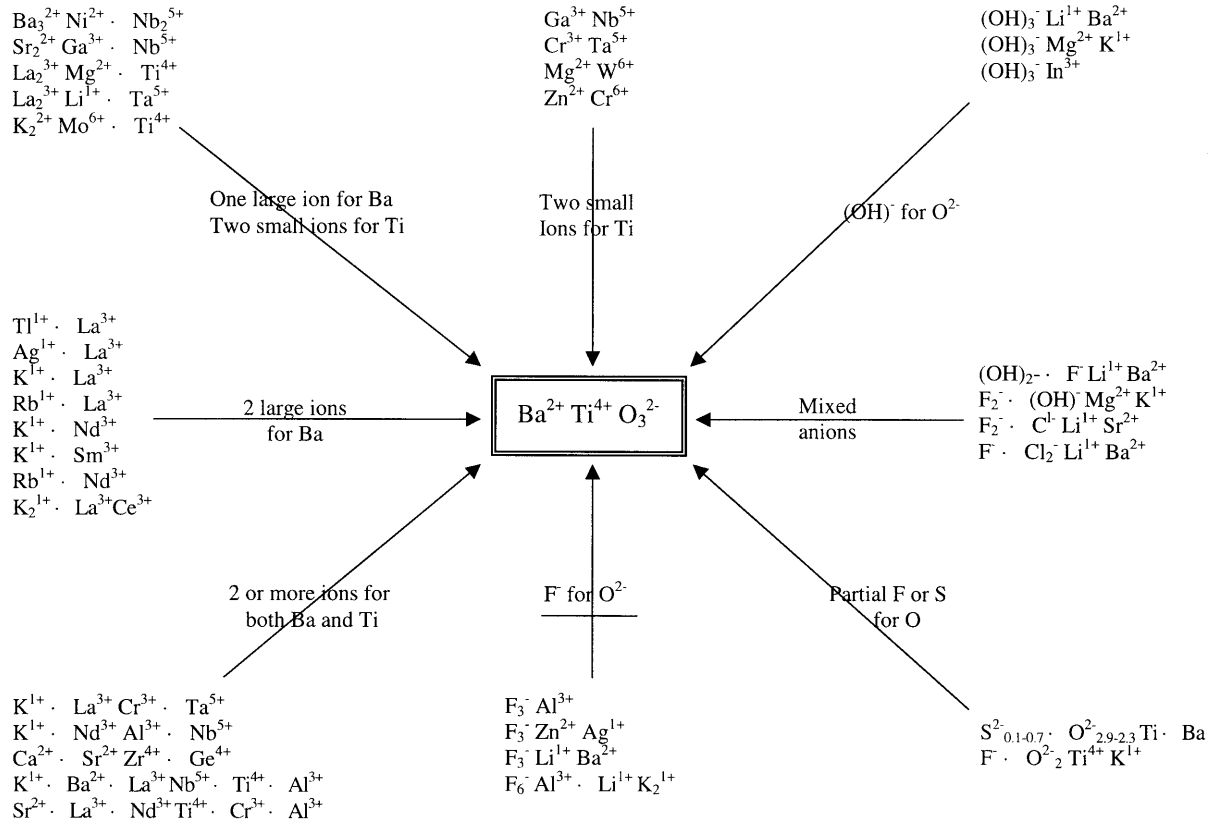

Fig. 3 Crystal chemistry of multiple ion substitution in perovskite (Roy 1954)

sic advance not envisaged by Goldschmidt. Thus Roy et al. were able to make many "half-breed derivatives" on the A site, B site, and mixed (M.J. Buerger terminology).

Figure 3 is taken from Roy's summary of this work in 1954 [42]. This list of materials synthesized, viewed in retrospect is remarkable. The prototype of virtually every useful substitution made in the perovskite structure is illustrated by *real* examples in this figure. For example, the $A_3B^{2+}B_2^{5+}O_9$ is the prototype of the PMN relaxor material, typified by its prototype $Sr_3NiNb_2O_9$. This map serves even today as a template for the novice interested in introducing any particular ion into the perovskite structure. The one major limitation is that unlike the garnet and spinel structures, no small ions <≈0.6 A can be accommodated since there are no tetrahedral sites in the perovskite structure.

But just as Goldschmidt had worked on the relations of two structures [Perovskite] – [Ilmenite], [NaCl] – [CsCl], etc., Roy turned his attention to the general problem of how structures of ternary phases change with the cation radius of the two ions involved. His very first work was on the ABO_3 phases (Keith and Roy [43]) and in this paper the first (crude) examples of Structure Field Maps are presented, showing the relation of perovskite to neighboring structures; and it was in this paper that the discovery of ferromagnetic rare earth garnets was first reported.

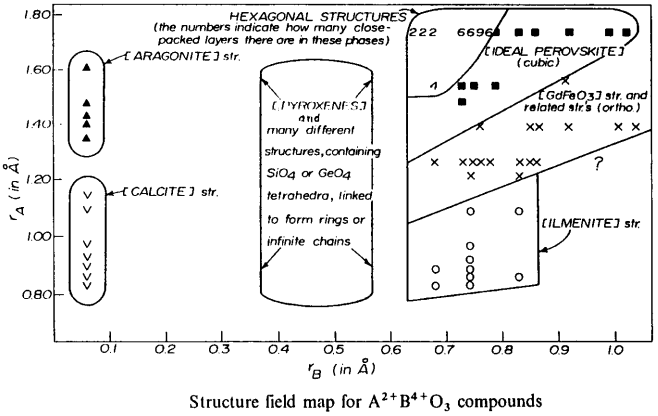

Structure field map for $A^{2+}B^{4+}O_3$ compounds

Fig. 4 Structure-field map for $A^{2+}B^{4+}O_3$ compounds

2.2.1 Structure field maps

In the subsequent decades Roy and his students developed the Goldschmidt approach much further and produced a large number of "structure field maps." The limitations of such an approach are clearly recognized. The zeroth order approximation of the structure of a real material is a hard sphere model, with each ion having simple integral charges involving only *s* and *p* electrons in purely electrostatic bonding. Of course none of these boundary conditions exists in practice, but nevertheless the deviations prove to be minor. The absolute dominance of composition on structure, as indicated by Goldschmidt, is demonstrated by the segregation of allowed

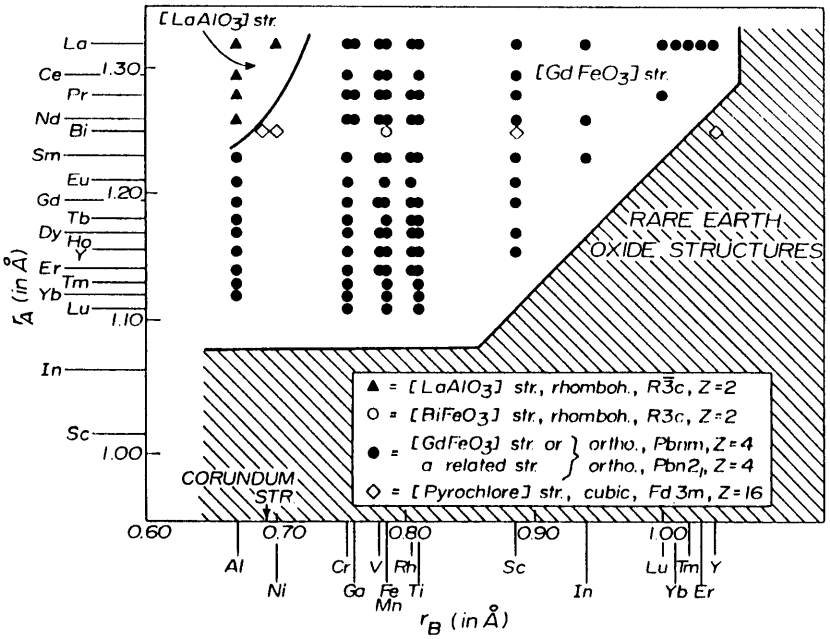

Structure field map for $A^{3+}B^{3+}O_3$ [perovskites]

Fig. 5 Structure-field map for $A^{3+}B^{3+}O_3$ [perovskites]

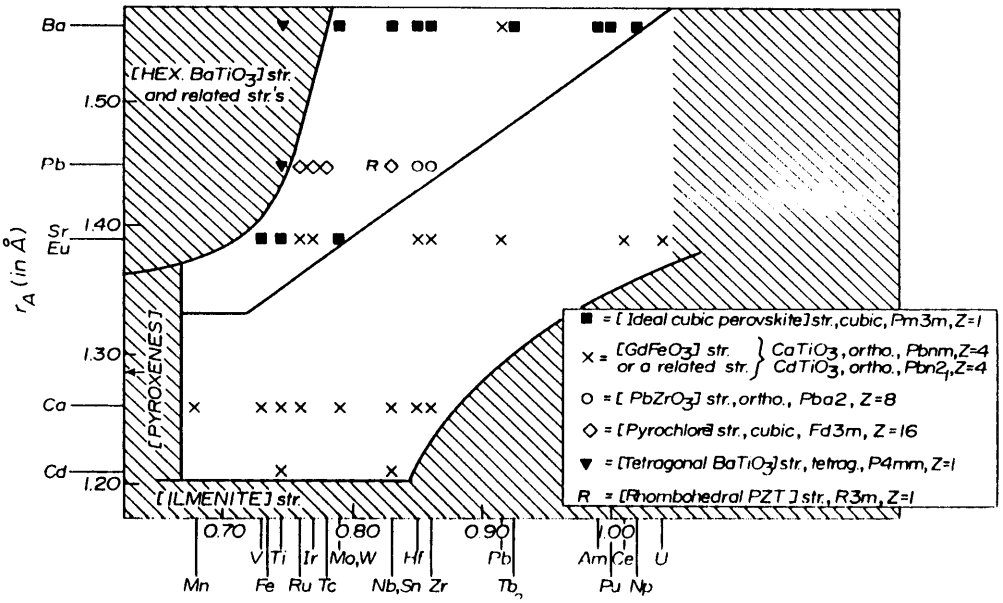

Structure field map for $A^{2+}B^{4+}O_3$ [perovskites]

Fig. 6 Structure-field map for $A^{2+}B^{4+}O_3$ [perovskites]

structures for any particular stoichiometry: ABX_3, A_2BX_4, ABX_4, etc. Among all ternary phases the actual numbers of structures are possible very limited. Ninety-five percent of all such phases on the earth probably fall into less than a couple of dozen structures. In their book "The Major Ternary Structural Families" Muller and Roy [1] have collected such information into one place and presented dozens of such structure field maps. Galasso [44] has also provided a valuable similar compilation of data. Figs. 4–6 show the kind of information which is conveyed in such SFM. These maps show the extent of the domain of occurrence of a particular structure or substructure (for example rhombohedrally on tetragaonally distorted perovskites) in radius space of the two cations A and B in any ternary phase. While from Goldschmidt's earliest work it was clearly recognized that the effect of radius was modulated by "polarization," or what became in Pauling's approach the "percentage covalency (ionicity)." So far it has not been usefully reduced to simple presentations in complex ionic compounds. In the simpler case of metallic structures it was Brewer and Engels [45] who took this approach by adding in a term for the

effects of '*d*' and '*f*' electrons participating in the bonding. In the "covalent" approximation to carbon, silicon, germanium and the partially ionic III-V and II-VI compounds, the theoretical physics community (A. Zunger [46]; J.C. Phillips [47, 48]) has attempted (what are labeled) "first principles" calculations to relate composition to structure. After enormous efforts, the results are marginally more precise than Goldschmidt's 1926 results which require no more effort than reading off radii from a table. Moreover, virtually no such efforts have been attempted for ternary or quaternary structures.

2.2.2 Point defects – substitution (solid solutions) and vacancies

The only defects which affect the bulk crystal structure are those which affect the chemical composition. *Solid* (more accurately, *crystalline*) solutions are universal. All solid matter deviates (i.e., is defective), with respect to the deviation of ionic content, from the formal ratios of say 1:1:3 in ABX_3. In many well-known structures (e.g., in the case of $TiO_{(1\pm x)}$ the deviation can be 20–30 percent). In perovskite it can be 100%. Thus the phase ReO_3 should be written $Re^{6+}O_3^{2+}$, because while its structure is that of perovskite, the A sites are 100% vacant. The so-called tungsten bronzes based on "$NaW^{5+}O_3$" in fact are heavily defective (i.e., lacking in A ions) along a formula which simply drops out Na^{1+} ions, $Na_{1-x}\ W^{5+}_{1-x}\ W^{6+}_{x}\ O_3$ by balancing out the partial oxidation of W^{5+} to W^{6+}. A special category of 'defect' that Goldschmidt recognized was the charge "model." He argued that if one dropped the formal charge of O^{2-} to F^-, one could substitute K^+ for Ba^{2+} and Mg^{2+} for Ti^{4+} and retain the perovskite structure. Indeed the prediction of the structures of chemically utterly different phases such as $KMgF_3$, Na_2BeF_4 and BeF_2 by involving the model structure theory must be regarded as one of the spectacular triumphs of crystal chemistry – and this was 1926.

The immeasurable number of solid solutions, which are used in technology daily, are quite simply limited by the radius considerations in the structure field maps. Especially relevant often are cases where a designed composition may switch from the pyrochlore to the perovskite structure [1] as the defect concentration changes (see examples in [50]).

2.2.3 Defects: Order-disorder

Another important consideration in complex-composition perovskites are in the half-breed compositions of Roy [42]. Here say $K^{1+} + La^{3+}$ are substituted for $2Ba^{2+}$; or $Mg^{2+} + Nb_2^{5+}$ are substituted for $3Ti^{4+}$. The possibilities of order-disorder structural changes become obvious. In the disordered state the ions are statistically distributed over the 2 (or 3) A (or B) sites. However at lower temperature, a lower free energy possibility is often assured whereby a superstructure is formed with a larger unit-cell and the ions segregated into chemically homogeneous sublattices. These order-disorder changes cause very significant electrical and optical changes and the systematization is very valuable.

2.3 Phase diagrams: Stable and metastable

While crystal chemistry relates composition to structure, thermodynamics relates structure and composition to the intensive variables principally of temperature and pressure. It is a fact that in contradistinction from other structures say [NaCl] or [Diamond], the usual laboratory pressure variable (up to say 100 kbars) causes virtually no phase transition in any perovskites; (see later for $MgSiO_3$ in the earth) hence it is only the T-x diagrams which are of interest to the perovskite field for synthesis and growth and solid solutions etc. The original T-x diagram for the system $BaO\text{-}TiO_2$ was done by Rase and Roy in 1954 [51]. It is shown in Fig. 7(a), alongside the much later one [52] [Fig. 7(b)] the significant changes are all in the high TiO_2 region where some new phases have been detected, which resulted in very minor changes in the melting temperatures involved.

3 Major applications in electroceramics

As mentioned earlier (Fig. 2) in an ideal perovskite structure the corner-shared oxygen octahedra linked in the three dimensions is the basic feature of the perovskite structure. The origin of ferroelectricity is linked with the characteristics of the oxygen octahedron unit not only in this structure but also in other derivative structures, e.g., tungsten bronzes and the bismuth titanate structure. Within the perovskite subgroup there are many possible variations of ferroics and phase transitions, e.g., ferroelectric, antiferroelectric, ferroelastics (Table 5 [53]).

In a simple composition when the octahedra are linked in a regular fashion in a cubic material a high temperature or prototype m3 m point symmetry perovskite is formed. Various A-site substitutions result in a large family of simple perovskite ferroelectrics, which at present numbers over 100 ferroelectrics. The variation of these corner linked octahedra such as tilt, (1,2,3 axis) [54] rotations give the possibility of several new families of ferroelectrics. Two of those which are worth mentioning here are the tungsten bronze structure (tilting of the octahedra in the a-b plane) and Bi-layer structures (where corner linked oxygen octahedra layers are separated by $Bi_2O_2^{+2}$ layers in the structure). The former family has about the same number of solid solution ferroelectric tungsten bronze compositions and the latter one, well over 50 compounds though the number increases to very large numbers when these are modified or the solid solution compositions are designed by using the simple principles of crystal chemistry.

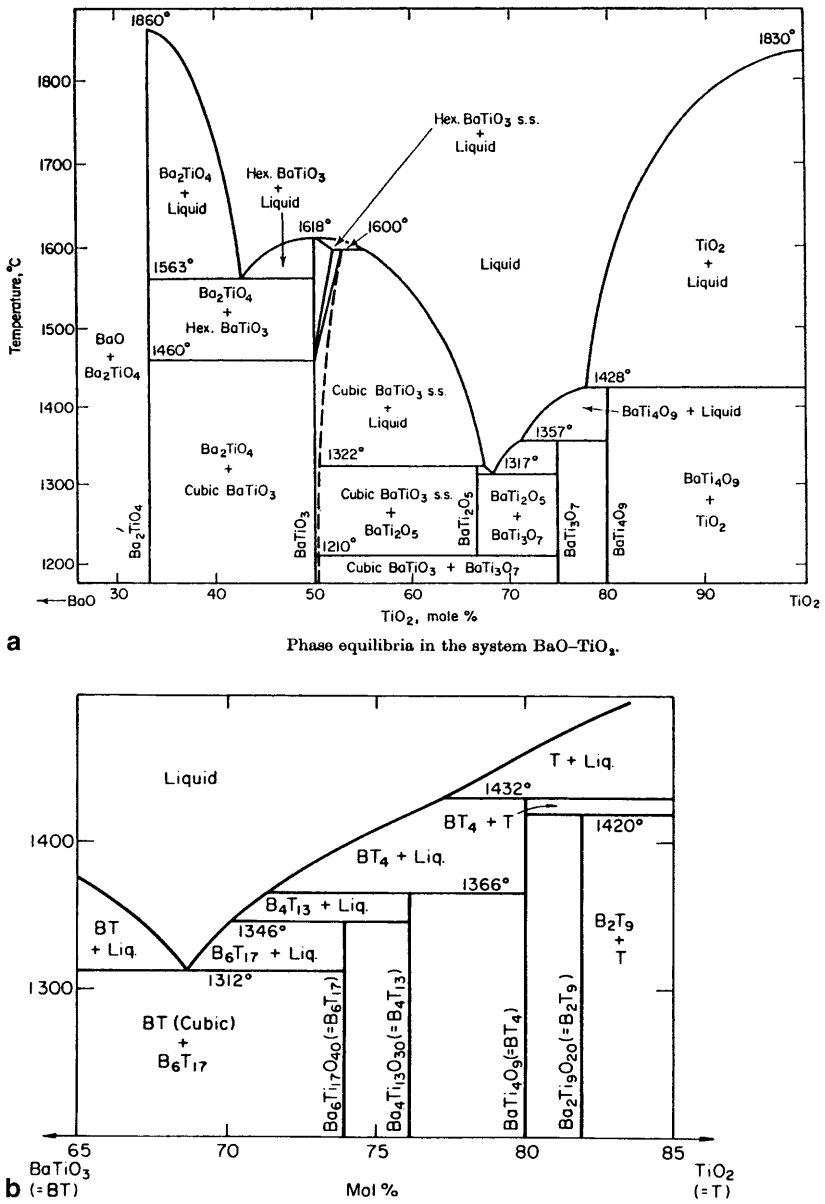

Fig. 7 (**a**) Phase equilibria in the system BaO-TiO_2 (Rase and Roy 1954); and (**b**) later version of the diagram (ref [52])

Table 5 Primary and secondary ferroics (Newnham and Cross)

Ferroic class	Orientation states differ in	Switching force	Example
Primary:			
Ferroelectric	Spontaneous polarization	Electric field	$BaTiO_3$
Ferroeleastic	Spontaneous strain	Mechanical stress	$CaAl_2Si_2O_8$
Ferromagnetic	Spontaneous magnetization	Magnetic field	Fe_3O_4
Secondary:			
Ferrobielectric	Dielectric susceptibility	Electric field	$SrTiO_3$ (?)
Ferrobimagnetic	Magnetic susceptibility	Magnetic field	NiO
Ferrobielastic	Elastic compliance	Mechanical stress	SiO_2
Ferroelastoelectric	Piezoelectric coefficients	Electric field and mechanical stress	NH_4Cl
Ferromagnetoelastic	Piezomagnetic coefficients	Magnetic field and mechanical stress	$FeCO_3$
Ferromagnetoelectric	Magnetoelectric coefficients	Magnetic field and electric field	Cr_2O_3

In the simple ferroelectrics (at room temperature) the origin of ferroelectricity in the high symmetry paraelectric perovskite is governed by the two unequal TiO^1 and TiO^2 (and thus reduction of m3 m symmetry to 4 mm) bond distances. At a suitable temperature (Tc) when TiO^1=TiO^2, the distorted perovskite (or ferroelectric) transforms back to the cubic high symmetry m3m perovskite structure.

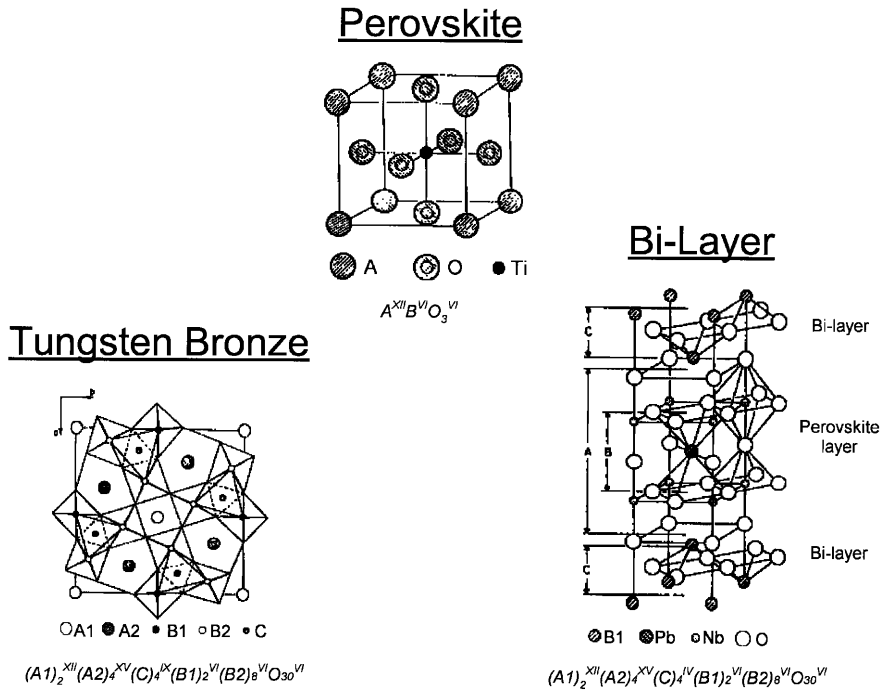

Fig. 8 Other variants of perovskite structure

Table 6 Prime device materials in the field of electroceramics

Device applications	Perovskite materials
Microwave dielectrics	$Ba(Zn_{1/3}Nb_{2/3})O_3$, $Ba(Mg_{1/3}Ta_{2/3})O_3$ and Large number of modified compositions
Microwave dielectric substrates for HTSC	$LaAlO_3$, $NdGaO_3$, $Sr(Al_{0.5}Ta_{0.5})O_3$, $Sr(Al_{0.5}Nb_{0.5})O_3$
NOx sensors	$LaFeO_3$
Dielectric resonators	$BaZrO_3$
Resistors	$BaRuO_3$
Conducting electrodes	$SrRuO_3$, $LaCoO_3$
Superconductors	YBCO, BiSCO, $Ba(Pb,Bi)O_3$
Laser host	$YAlO_3$
Magnetic bubble	$GdFeO_3$
Ferromagnetics	$(Ca,La)MnO_3$

Table 7 Some of the practical uses of simple ferroic perovskites and their solid solutions (non ferroelectric and ferroelectrics) are listed

Ferroic perovskite	Comments/applications
$BaTiO_3$	Capacitors, PTC (for hair driers, etc.)
$PbTiO_3$	Pyroelectric detectors, hydrophone, high d_hg_h, d_h
$Pb(Zr_{1-x}Ti_x)O_3$	Piezoelectric applications of all kind. Simple modifications of compositions or dopants are used for obtaining the suitable material for a specific application, e.g., transducers, hydrophones, actuators, x-y translator, e.g., AFM
$PbLa(ZrTi)O_3$ –8/65/35	Transparent ceramics, electrooptic shutters, EO goggles, etc. for high altitude flying pilots
$LiNbO_3$	Variant of perovskite: Optical modulators
$LiTaO_3$	Variant of perovskite: pyroelectric sensors
$KNbO_3$	Best second harmonic generator
Doped Rh: $BaTiO_3$, $KNbO_3$, Fe:$LiNbO_3$	Photorefractive materials
$SrTiO_3$, ($KTaO_3$)	Tunable microwave devices

There are some other variants of the perovskite structures with other special arrangements (Fig. 8) and which have the limited number of compounds. $LiNbO_3$ and $LiTaO_3$ and their solid solutions along with a few substituents are the most important materials. Because of the versatility of the perovskite structure in exhibiting the vast range of conduction behaviors (as shown below),

Insulator	FE	AFE	Conductor	Superconductor
$SrTiO_3$	$BaTiO_3$	$NaNbO_3$	$La(Cr,Mn, Ni)O_3$	YBCO, etc.

Table 8 Comparison of relaxor and normal ferroics

Property	Normal	Relaxor
Permittivity temperature dependence	Sharp 1st or 2nd order transition about Curie temperature (T_c)	Broad-diffuse phase transition $\varepsilon=\varepsilon(T)$ about Curie maxima (T_{max})
Permittivity temperature and frequency dependence $\varepsilon=\varepsilon(T, \omega)$	Weak frequency dependence	Strong frequency dependence
Permittivity behavior in paraelectric range ($>T_c$)	Follow Curie-Weis law Equation: $1/K=C/(T-T_c)$	Follow Curie-Weis square law Equation: $1/K=1/K_{max}+(T-T_{max})^2/2K_{max}\delta^2$
Remanent polarization	Strong remanent polarization	Weak remanent polarization
Scattering of light	Strong aniostropy (birefringent)	Very weak anisotropy to light (pseudo-cubic)
Diffraction of x-rays	Line splitting owing to spontaneous deformation from paraelectric to ferroelectric phase	No x-ray line splitting giving a pseudo-cubic structure

the compounds of this family are the prime device materials in the field of electroceramics (Table 6). Some of the practical uses of these simple ferroic perovskites and their solid solutions are listed in Table 7.

3.1 Relaxors

A special family of substituted perovskites which have extraordinarily high dielectric constants have been called "relaxors." From the crystal chemistry point of view the perovsktie structure can accept a large number of ionic substitutions to form new simple or complex compounds as well as solid solutions amongst the various oxide or complex oxide compositions (Fig. 9). In particular lead based complex perovskites with the formula $PbA'BO_3$, $PbB'B''O_3$, $PbA'B'B''O_3$ where $A'=La^{3+}$, etc., $B'=Fe^{2+}$, Mg^{2+}, Zn^{2+}, In^{3+}, Sc^{3+}, and $B''=Nb^{5+}$, Ta^{5+}, W^{6+} result in nanoscale ordered regions in a disordered matrix (Fig. 10). In some cases the material can be converted in to an ordered state. Also the characteristics of the substitutions are not limited to the ionic species listed above but these are some which so far have been prepared, studied, and used in a wide range of applications. The degree of ordering in some of these materials can be adjusted by simple processing and thermal annealing approach whereas in most materials the structure remains in the highly disordered state. These materials have some characteristics which normal perovsktie ferroelectrics do not exhibit (Fig. 11). Table 8 shows the comparison of relaxor and normal ferroics.

All the unusual characteristics observed in these materials have been associated with the order-disorder behavior and the degree of order present in these materials. Also perovskites (and some of the related tungsten bronze structure materials) are the only materials so far which have demonstrated this characteristic. Such ferroelectric compositions are categorized as "relaxor ferroelectrics" [55, 56]. Structurally most perovskite based relaxors, due to the presence of slight lattice distortion are in the rhombohedral symmetry. Relaxor materials have shown great promise in most ferroelectric-related application arenas (Table 9).

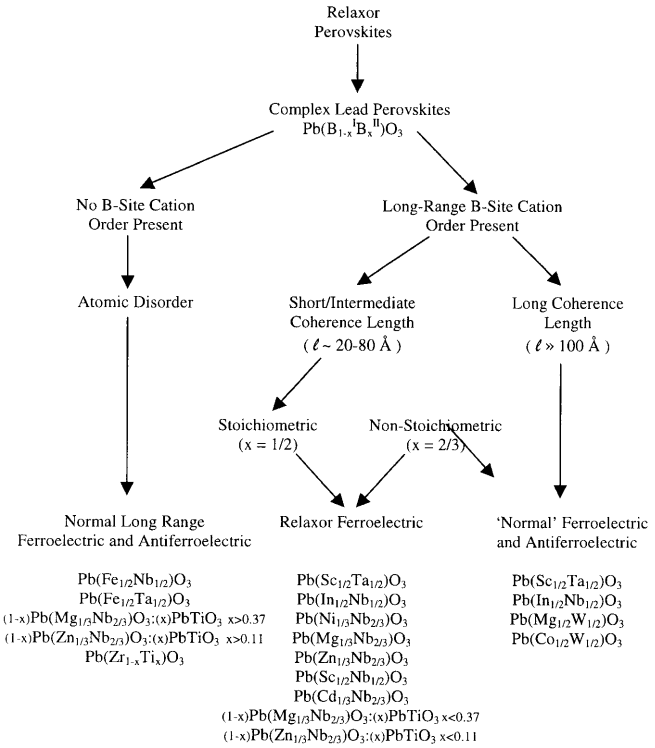

Fig. 9 Various relaxors perovskite combinations and their classification based on short and long range ordering (after Randall and Bhalla)

3.2 Morphotropic phase boundary compositions

It is quite interesting to note that a further expansion of the perovskite ferroelectrics list is possible by the route of solid solution between various classes of perovskite ferroelectric and relaxor (Table 10; [57, 58]). In most cases a morphotropic phase boundary [59] (Fig. 12) occurs at which point several ferroelectric properties change drastically in favor of device applications (Table 11; [56]).

The morphotropic phase boundary (MPB) represents an abrupt structural change within a solid solution with variation in composition but nearly independent of temperature. Usually it occurs because of the instability of one phase against the other at a critical composition

where two phases are energetically very similar but elastically different. It is noticed that the dielectric constant, piezoelectric and electromechanical characteristics, spontaneous polarization and pyroelectric behavior attain maxima whereas the elastic constants tend to be softer in the vicinity of the MPB. Because of such high property coefficients and unique structural characteristics of MPB compositions, a vast number of publications and patents (Table 12) covering various device applications of this class of ferroelectric have been added in the field of electroceramics. Bhalla et al. [60] have recently compiled the vast literature on the structure property diagrams of the relaxor MPB systems. Figure 13 shows the current trend and increased interest in the relaxor based MPB systems [60].

3.3 Microwave dielectrics

Dielectric resonators are the prime components in various communication and microwave systems as those provide for very effective size reduction for microwave components (size $\propto 1/\sqrt{\text{dielectric constant}}$) compared to that for air filled cavities. In such applications, the material should fulfill the following stringent requirements (Table 13): (1) high dielectric constant, κ (at microwave frequencies); (2) minimum possible dielectric loss, tanδ; (3) temperature stability of the dielectric properties; (4) very low thermal expansion coefficients (which is related to (3)).

In a high quality microwave dielectric material the requirements (2), (3) and (4) should be as close to zero as possible. To have such an ideal material available is highly improbable, but suitable materials can be de-

Table 9 Areas of applications for relaxor ferroelectrics and solid solutions

Application:	Example:
Pyroelectrics	$Pb(Sc_{1/2}Ta_{1/2})O_3$ $(Ba_{0.60}Sr_{0.40})TiO_3$
Capacitors/dielectrics	$Pb(Mg_{1/3}Nb_{2/3})O_3$ (see patent list)
Electrostriction/actuators	$Pb(Mg_{1/3}Nb_{2/3})O_3$ $Pb(Zn_{1/3}Nb_{2/3})O_3$ $Pb[(Mg_{1/3}Nb_{2/3})_{1-x}Ti_x]O_3$
Medical ultrasound/high efficiency transducers	$Pb[(Zn_{1/3}Nb_{2/3})_{1-x}Ti_x]O_3$ $Pb[(Sc_{1/2}Nb_{1/2})_{1-x}Ti_x]O_3$
Piezoelectrics	$Pb(Zr_{1-x}Ti_x)O_3$ $Pb[(Zn_{1/3}Nb_{2/3})_{1-x}Ti_x]O_3$ $Pb[(Sc_{1/2}Nb_{1/2})_{1-x}Ti_x]O_3$
Electrooptics	$(Pb_{1-x}La_{2x/3})(Zr_{1-y}Ti_y)O_3$

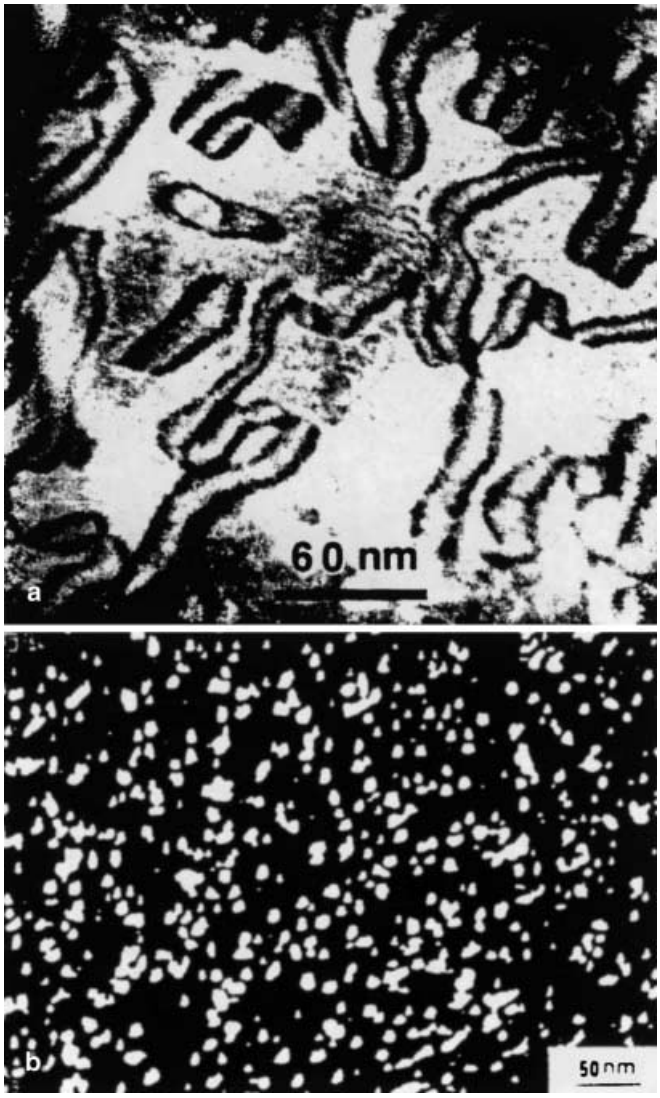

Fig. 10a, b Nanoscale ordered regions in a disordered matrix. (**a**) $PbSc_{1/2}Ta_{1/2}O_3$ (Harmer, Bhalla); and (**b**) $PbMg_{1/3}Nb_{2/3}O_3$ (Randall et al.)

Table 10 Summary of important relaxors based on MPB systems (Bhalla et al.)

System:[a]	Example:
Antiferroelectric : proper ferroelectric	$PbZrO_3 : PbTiO_3$
Relaxor : proper ferroelectric	$Pb(Zn_{1/3}Nb_{2/3})O_3 : PbTiO_3$
Relaxor (short range order) : proper ferroelectric	$Pb(Mg_{1/3}Nb_{2/3})O_3 : PbTiO_3$
Relaxor (order-disorder) : proper ferroelectric	$Pb(Sc_{1/2}Nb_{1/2})O_3 : PbTiO_3$
Relaxor : antiferroelectric	$Pb(Zn_{1/3}Nb_{2/3})O_3 : PbZrO_3$
Relaxor (short range order) : relaxor (order-disorder)	$Pb(Mg_{1/3}Nb_{2/3})O_3 : Pb(Sc_{1/2}Nb_{1/2})O_3$
Relaxor (o – d) : relaxor (o-antiferroelectric – d-ferroelectric)	$Pb(Sc_{1/2}Ta_{1/2})O_3 : Pb(In_{1/2}Nb_{1/2})\ O_3$
Relaxor (sro) : relaxor (o-antiferroelectric – d-ferroelectric)	$Pb(Mg_{1/3}Nb_{2/3})O_3 : Pb(In_{1/2}Nb_{1/2})\ O_3$

[a] o: order, d: disorder, sro: short range order

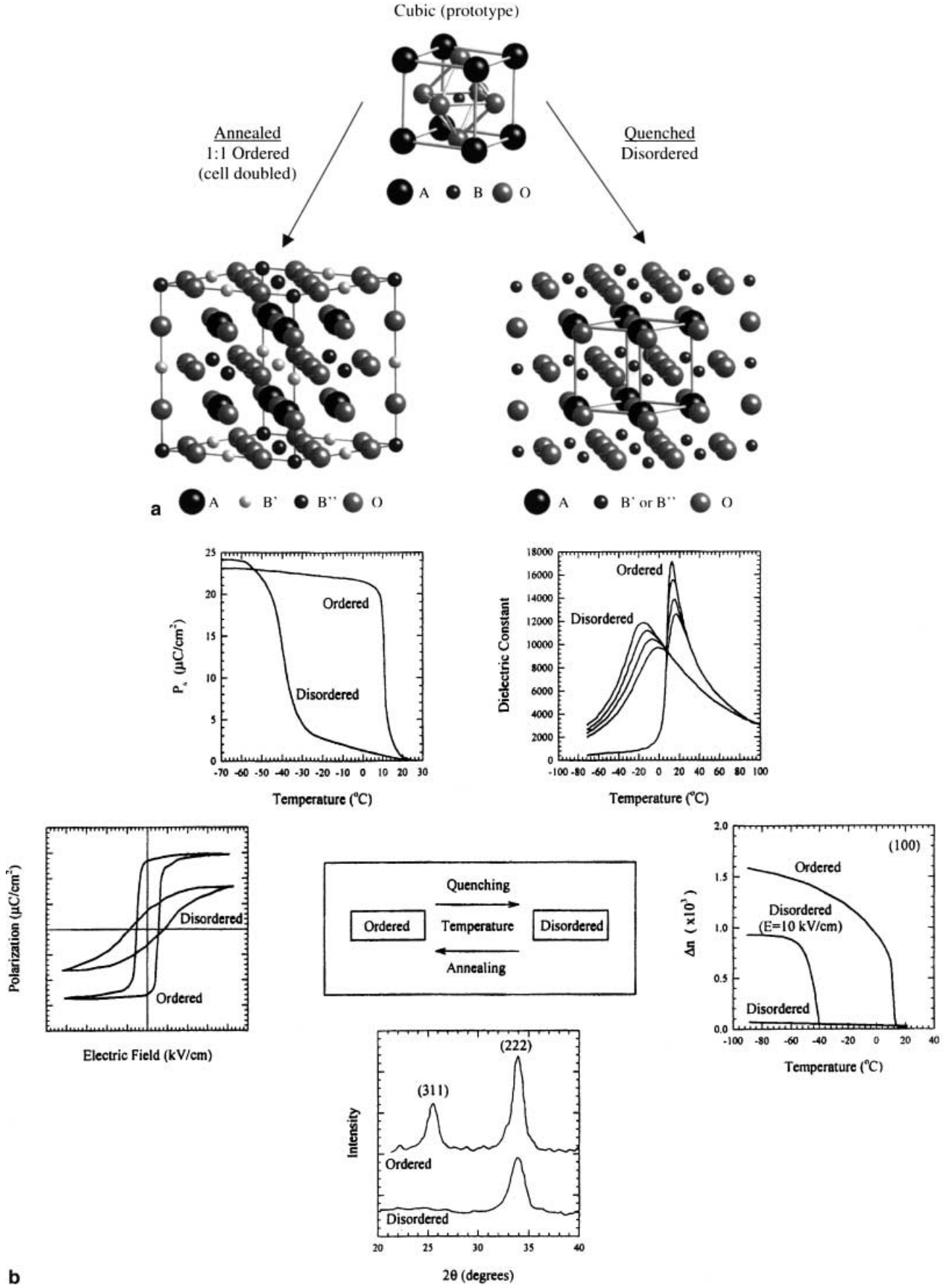

Fig. 11 (**a**) o-d structure in perovskites, and (**b**) properties in relation to o-d structure

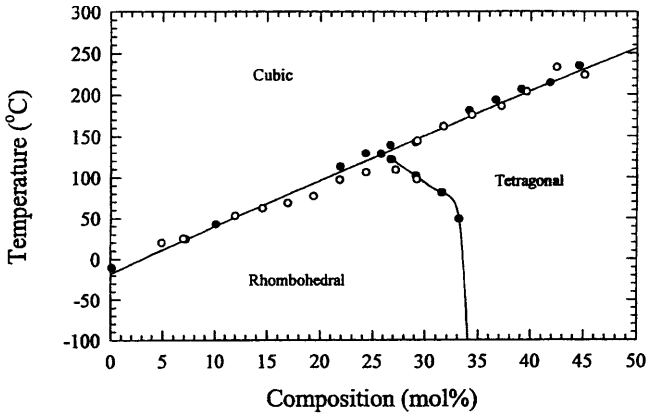

Fig. 12 Phase diagram for the (1-*x*)PMN:xPT system (Choi et al.)

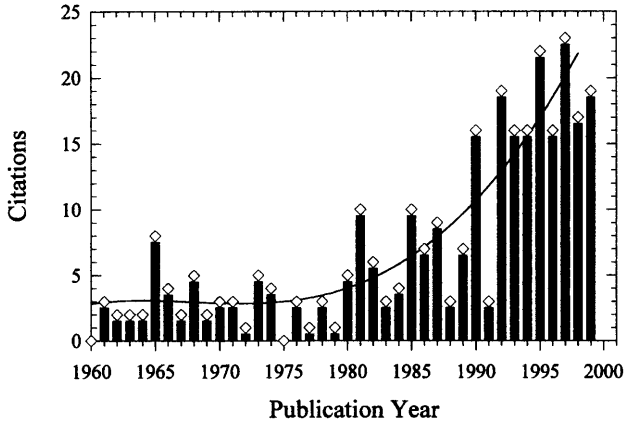

Fig. 13 Number of new relaxor-based solid solution citations reviewed by year

Table 11 Commonly employed perovskite end members for relaxors

Complex perovskites	T_c (°C)	Behavior[a]	Simple Perovskites	T_c (°C)	Behavior
$Pb(Mg_{1/3}Nb_{2/3})O_3$	–10	RFE	$PbTiO_3$	190	FE
$Pb(Zn_{1/3}Nb_{2/3})O_3$	140	RFE	$PbZrO_3$	230	AFE
$Pb(Ni_{1/2}Nb_{1/2})O_3$	–120	RFE	$BaTiO_3$	130	FE
$Pb(Fe_{1/2}Nb_{1/2})O_3$	110	FE	$SrTiO_3$	–	PE
$Pb(Fe_{2/3}W_{1/3})O_3$	–95	RFE			
$Pb(Mg_{1/2}W_{1/2})O_3$	38	AFE			
$Pb(Nb_{1/2}W_{1/2})O_3$	17	AFE			

[a] FE: ferroelectric, AFE: antiferroelectric, RFE: relaxor-ferroelectric, PE: para-electric

Table 12 List of a few relaxor-based compositions for MLC

Composition	EIA specification	Manufacturer	Patents
PLZT-Ag	X7R	Sprague	U.S. Pat. 4,027,209 (1973)
PMW-PT-ST	X7R	DuPont	U.S. Pat. 4,048,546 (1973)
PFN-PFW	Y5V	NEC	U.S. Pat. 4,078,938 (1978)
PFN-PFW-PZN	Y5V	NEC	U.S. Pat. 4,236,928 (1980)
PFN-PMT	–	TDK	U.S. Pat. 4,216,103 (1980)
PMN-PT	Y5V	TDK	U.S. Pat. 4,265,668 (1981)
PMN-PFN	Y5V	TDK	U.S. Pat. 4,216,102 (1980)
PMN-PFN-PMW	Y5V	TDK	U.S. Pat. 4,287,075 (1981)
PFW-PZ	Z5U	TDK	U.S. Pat. 4,235,635 (1980)
PFW-PT-MN	Z5U	Hitachi	U.S. Pat. 4,308,571 (1981)
PMN-PZT-PT	Z5U	Murata	U.S. Pat. 4,339,544 (1982)
PFN-PFW-PbGe	X7R	–	–
PFN-PFM-PNN	Z5U, Y5V	Ferro	U.S. Pat. 4,379,319 (1983)
PMW-PT-PNN	Z5U	NEC	U.S. Pat. 4,450,240 (1984)
PFN-BaCa(CuW)-PFW	Y5V	Toshiba	U.S. Pat. 4,544,644 (1985)
PMN-PZN	Z5U	STL	U.K. Pat. 2,127,187A (1984)
PMN-PFN-PT	Z5U	STL	U.K. Pat. 2,2126,575(1984)
PMN-PZN-PFN	Z5U	Matshshita	Japan Pat. 59–107959 (1984)
PMN-PFW-PT	–	Matshshita	Japan Pat. 59–203759 (1984)
PNN-PFN-PFW	Y5V	Matshshita	Japan Pat. 59–111201 (1984)
PZN-PT-ST	–	Toshiba	–
PMN-PFN-PbGe	Z5U	Union Carbide	U.S. Pat. 4,550,088 (1985)
PFN-PNN	Y5V	–	–
PFW-PFN	–	NTT	–
PMN-PT-PNW	Z5U	Matshshita	–
PMW-PT-PZ	X7R	NEC	–
PZN-PMN-PT-BT-ST	Z5U	Toshiba	Japan Pat. 61–155245 (1986)
PZN-PT-BT-ST	X7R	Toshiba	Japan Pat. 61–250904 (1986)
PZN-PMN-BT	Z5U, Y5S	Toshiba	–
PMN-PLZT	Z5U	MMC	U.S. Pat. 4,716,134 (1987)
PMN-CT,ST,BT	Z5U	Matshshita	Japan Pat. 62–115817 (1986)
PFW-PFN-PT	Y5V	–	–
BT-PMN-PZN	X7R, X7S	Toshiba	U.S. Pat. 4,767,732 (1988)
PMN-PS-PNW-Ca	–	–	–
(base metal)	Z5U	Matsushita	–

Table 13 Microwave dielectrics (a) and (b) (Table based on [64])

	ε_r	Q (4 GHz)	T_f	f_0 (GHz)	Q×f (×10^3)	Refs[a]
Temperature coefficients						
$Ba_2Ti_9O_{20}$	40	9000	+2			4, 5
$(Zr,Sn)TiO_4$	34–37	9000	+/–20			6
$(Sr,Ca)[(Li,Nb)Ti]O_3$	38–46	3500 at 9 GHz	+30/–70			7
$BaTi_4O_9$	38	8500	+15			4, 5, 8
$(Ca,Sr)(Ba,Zr)O_3$	29–32	2500 at 11 GHz	+/– 50			9
$MgTiO_3$	17	22000 at 7 GHz	–45			23, 24, 25
$CaTiO_3$	170	1800 at 7 GHz	+800			
Q×f characteristics						
$MgTiO_3$-$CaTiO_3$	21	8000		7	56	14
$Ba(Sn,Mg,Ta)O_3$	24	43,000		10	430	15
$Ba(Zn,Ta)O_3$	30	14,000		12	168	16, 17
$Ba(Zr,Zn,Ta)O_3$	30	10,000		10	100	17, 18
$(Zr,Sn)TiO_4$	38	10,300		5	51	19, 20
$Ba_2Ti_9O_{20}$	40	8000		4	32	21, 22
BaO-PbO-Nd_2O_3-TiO_2	90	5000		1	5	19, 23

[a] number refers to that of in original paper

signed by using the simple guidelines of crystal chemistry as described in the following sections 5.1 and 6, also in the paper by Guo et al. [61].

Several compounds such as TiO_2, spinels and perovskites (Table 13) have been examined for microwave dielectric resonators but the perovskites provided the wide range of suitable materials, possibility of tailoring the parameters to meet the device requirements. In addition, several approaches like eutectics, composites (macro, micro and nanoscale) [62, 63] and solid solutions have been made to design optimum materials for specific applications.

While telecommunications are revolutionizing our lifestyle, the demand for new microwave dielectrics with the multifunctionality-feature is also increasing. The present technology in addition to the above listed requirements, demands tunable microwave dielectrics. To our surprise, so far, it appears that it is the perovskite family which provides the best materials e.g., $SrTiO_3$, $KTaO_3$, $CaTiO_3$, and several solid solutions e.g., $(BaSr)TiO_3$, $(PbSr)TiO_3$ etc. and their doped and modified compositions, for the frequency and field agile microwave electronics.

4 Perovskites as superconductors

4.1 Conductors and superconductors

While for 30 years the perovskite structure dominate the world of dielectrics, it was soon noted that a combination of *4f* ions in the A-site, and *3d* ions in the B-site give rise to reasonably conducting phases, at room temperature and at very high temperatures. For example, $LaCrO_3$ was a typical candidate for MHD electrodes, Rao et al. [65] vigorously followed up on cuprate conductors including "$BaCuO_3$" phases. But it was not their argument which led to the first superconductive perovskite. In 1975, Sleight el al. [66] developed the highest temperature oxide superconductor in a $BaBiPbO_x$ perovskite. In the late seventies Gilbert [67] and Gilbert and Roy [68] performed the usual substitutions in the structure to see if the T_C could be raised. All substitutions lowered the T_C. A self-imposed constraint of not using Cu^{2+} because of the variability of valence states, had them avoid the winner. Bednorz and Muller's early work [69] was on the K_2NiF_4 structure and the first perovskite phase with T_C over 30K was $BaLaCuO_x$ [70]. When James Ashburn [71] at the University of Alabama (Wu [72]) by sheer empirical mixing of "rare earth" and Ba, Sr, and Cu oxides discovered the "YBC" superconductor in a mixture of "green and black phases" the authors did not immediately connect the perovskite phase to the high T_C. In the event a highly defective perovskite $YBa_2Cu_3O_{7-\delta}$ was identified as the true high T_C material. Since then some billions of dollars (literally) have been spent in sheer empirical substitution of every easily conceivable combination of ions – the best work following well established crystal chemical principles in the perovskite structure. It is unlikely that any structure will ever receive the same detailed chemical manipulation again. It is significant to note that in this enormous international search the principles of physics could contribute nothing. The highest T_C materials at present are BiSCO and Hg-HTSC and represent another intercalated family not much unlike the Roddlesden-Popper phases.

4.2 Perovskite substrates for high-T_C superconductors

While the search for new superconductors by crystal chemical manipulation was intense for a dozen years, and relatively obvious substitutions increased the T_C some 30 °C, the selection of useful substrate materials for the deposition of high T_C superconductors (HTSC) is of prime importance and is subjected to a number of more difficult constraints, and has received much less attention. In several microwave applications of the "ceramic dielectric substrates," important considerations have been given to the (a) materials' thermal properties such as thermal expansion and thermal conductivity, and (b) the electrical characteristics such as low dielectric loss, dielectric constants and dielectric coefficient with

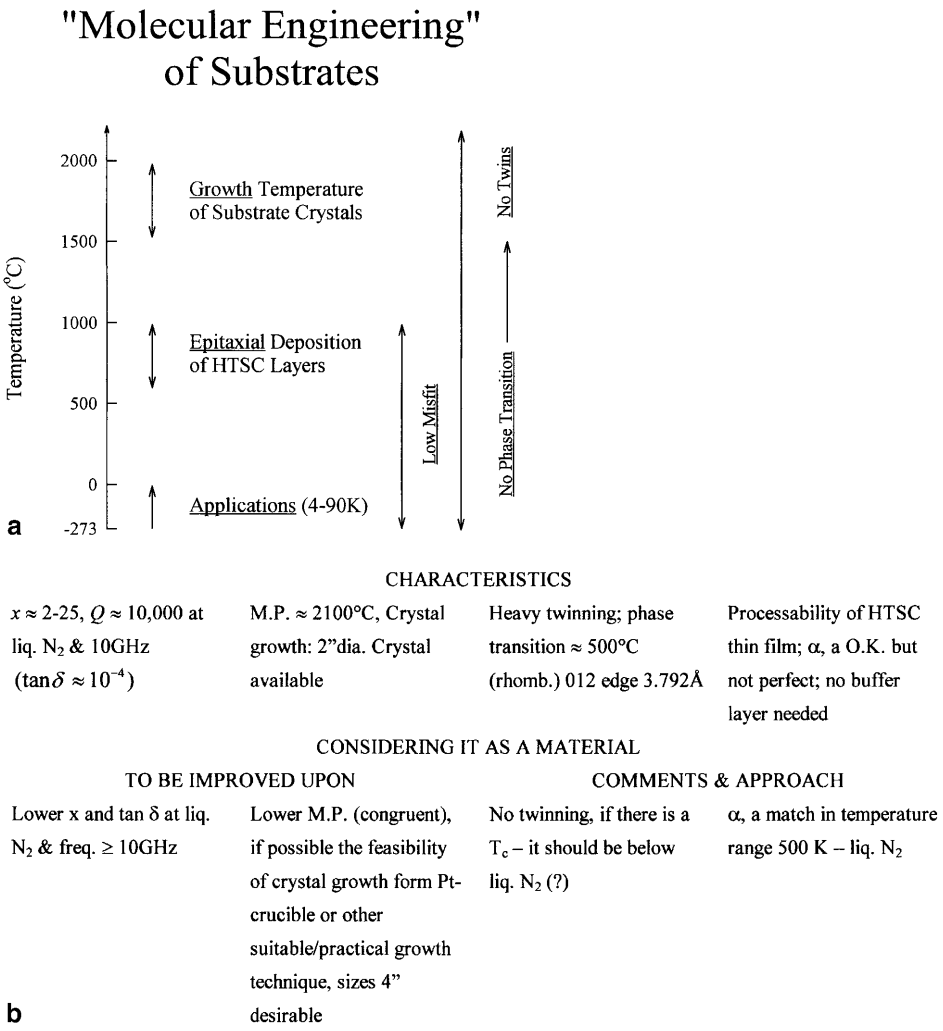

Fig. 14 (**a**) Temperature scale of substrates between their melting (growth) temperature and the application temperature (ranges 4 to 90 K). The regions of required low misfit and of required absence of twining due to structural phase transitions are indicated. (**b**) Structural and compatible aspects of substrates needed for the applications of HTSC films; selection criterion and improvement of substrate materials over the characteristics of well known $LaAlO_3$ crystals

Table 14 Substrate parameters required for HTSC film applications

	Multi-chip-modules (MCM)	Millimeter wave devices
Applications	Digital receivers, IR detectors, high performance computers	Oscillators; frequency discriminators; phase shifters; delay lines etc.
Requirements	High speed, $\nu\alpha 1/(x)^{1/2}$; satisfy characteristic impedance $1/Z\alpha(W/d)(x)^{1/2}$; high packing density (thinner film); low crosstalk (thinner film)	Narrow bandpass filters high Q); low temperature coefficient of capacitance; compact designs (moderate x values)
Dielectric constant	$x \approx 20$ or less is acceptable, however, for film thickness $d \approx 1$ μm, $x<10$ is required	$x \approx 20$–25 desirable
Dielectric loss	$\tan\delta<10^{-3}$ to maintain the dielectric loss much lower than the conductor loss	Ultra low loss, $\tan\delta<10^{-4}$ ($Q>10{,}000$)
Type of substrates	Single crystal films (2 μm) in multi-layer integrated structure with HTSC films	Single crystal substrates 3" or 4" in diameter

temperature. The main heart of the selection criteria are intended for the speed (in MCM devices) and the reduction of thermal effects on the signals. In case of the resonators the values of the constants are adjusted with the size of the required device. If we look for HTSC uses in such applications, the additional requirement from the substrates are also demanded. For example, additional crystallographic matching parameters are required to deposit high quality oriented (preferably epitaxial) and hence high J_C high temperature superconducting films on the single crystal perovskite substrates. These parameters are summarized in Table 14.

Table 15 Potential candidate materials for substrates for HTSC (Guo et al.)

Substance	@ 10 KHz, 90K	
	κ	D
$LaAlO_3$	21.5	7.47×10^{-5}
$Ba(Mg_{1/3}Ta_{2/3})O_3$		
hot-pressed ceramic	25.0	1.93×10^{-5}
ceramic	24.7	$<1\times10^{-5}$
crystal fiber	25.0*	$<1\times10^{-5}$
$(Ba_{0.9}Sr_{0.1})(Mg_{1/3}Ta_{2/3})O_3$	26.04	2.34×10^{-4}
$(Ba_{0.8}Sr_{0.2})(Mg_{1/3}Ta_{2/3})O_3$	26.6	1.96×10^{-4}
$MgLaAl_{11}O_{19}$	14.0	1.51×10^{-4}
$MgNdGaAl_{10}O_{19}$	15.6	1.75×10^{-4}
$CaGa_6Al_6O_{19}$	20.9	3.20×10^{-4}
$CaGa_{12}O_{19}$	9.4	1.81×10^{-4}
$Sr(Al_{1/2}Nb_{1/2})O_3$	18.7	2.20×10^{-4}
$Sr(Al_{1/2}Nb_{1/2})O_3$, Sol-Gel	17.2	6.57×10^{-4}
$0.7SAN:0.3LaAlO_3$	25.7	2.79×10^{-4}
$0.7SAN:0.3NdGaO_3$	23.0	5.15×10^{-4}
$Sr(Al_{1/2}Ta_{1/2})O_3$	11.8	4.24×10^{-5}
$Sr(Al_{1/2}Ta_{1/2})O_3$, Sol-Gel	11.5	6.05×10^{-4}
$0.7SAT:0.3LaAlO_3$	21.7	7.47×10^{-5}
$0.7SAT:0.3NdGaO_3$	16.0	4.25×10^{-4}
$1/3SAN:1/3SAT:1/3NdGaO_3$	22.3	5.11×10^{-4}
$La(Mg_{2/3}Ta_{1/3})O_3$	23.4	4.22×10^{-4}
$La(Mg_{1/2}Ti_{1/2})O_3$	27.1	1.82×10^{-4}
$La(Al_{1/4}Mg_{1/2}Ta_{1/4})O_3$	24.1	1.17×10^{-4}
$YBa_2Al_2TaO_9$	11.2	8.33×10^{-4}
$KMgF_3$	5.8	1.65×10^{-4}

Numerous candidate materials have been suggested for such purposes to achieve useful HTSC based devices. The most widely used candidate has been $LaAlO_3$. The serious problem of ferroelastic twinning in this material however, seriously affects the quality of HTSC film and the device performance. An additional factor, i.e., thermal expansion, must also be considered rather seriously in selection of the single crystal substrate materials for HTSC. In this case, the films are deposited and oxidized at ≈500 °C and the devices operate at liquid nitrogen temperatures. Therefore, for the lower aging effects and high performance from the device point of view, thermal expansion matching over the temperature range from the deposition temperature to liquid nitrogen are highly recommended. These features are illustrated in Fig. 14(a).

The goal has been to design and develop new highly suitable substrates which are better than that of $LaAlO_3$. Thus the considerations for the selection was based on the approach illustrated in Fig. 14(b) [73].

Investigations on the design and engineering of candidate substrate materials suitable for high T_C superconductor thin film deposition and application have yielded several interesting new hosts such as $Ba(Mg_{1/3}Ta_{2/3})O_3$ (BMT), $Sr(Al_{1/2}Ta_{1/2})_3$ (SAT); $Sr(Al_{1/2}Nb_{1/2})O_3$ (SAN). These complex perovskite phases and their associated solid solutions provide new options for ultra low losses; low permittivity substrates with close structural and thermal matching to the high T_C oxide superconductors. In this work it was necessary to develop a predictive capability for the dielectric constants of mixed oxide perovskites by extending Shannon's approach. Our approach is described later in Sect. 6.2 of this paper and some of the potential candidates developed are listed in Table 15.

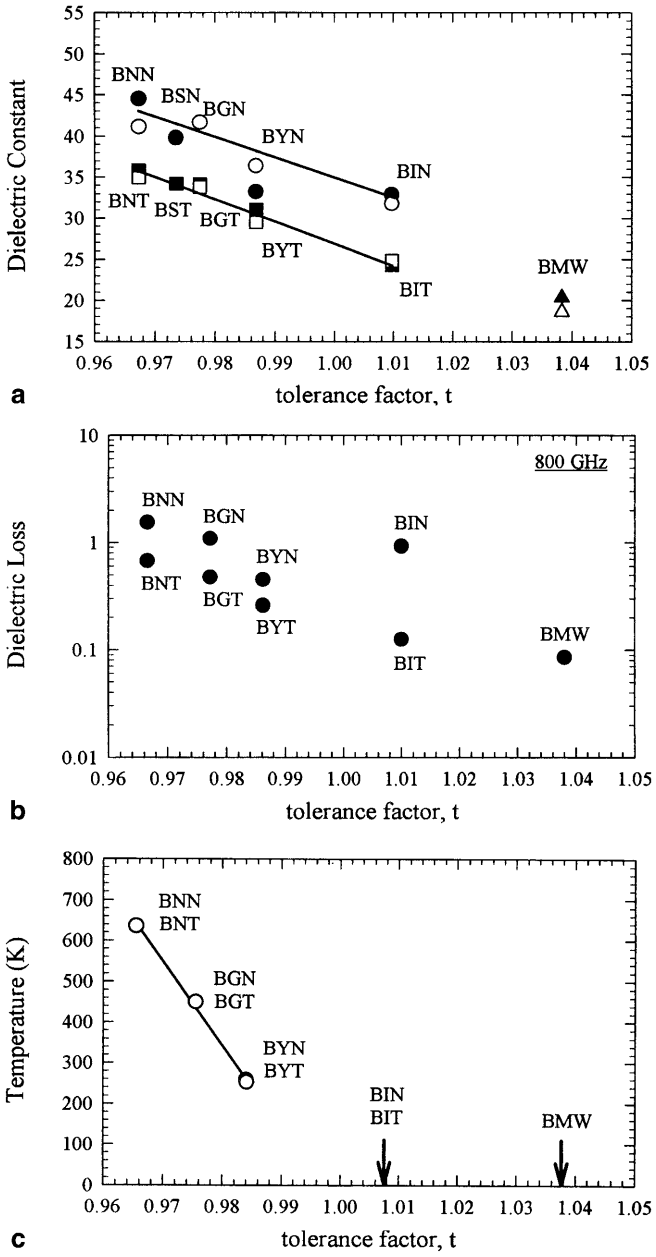

Fig. 15 (**a**) Dielectric constant vs. tolerance factor (Zumuhlen); (**b**) Dielectric loss vs. tolerance factor (Zumuhlen); and (**c**) Transition temperature vs. tolerance factor

5 Some specific features

5.1 Revisiting the tolerance factor and its new and added significance

The tolerance factor (T.F.), a simple geometrical number which was worked out by Goldschmidt, appears now to be a very useful figure. Recently, in trying to control the

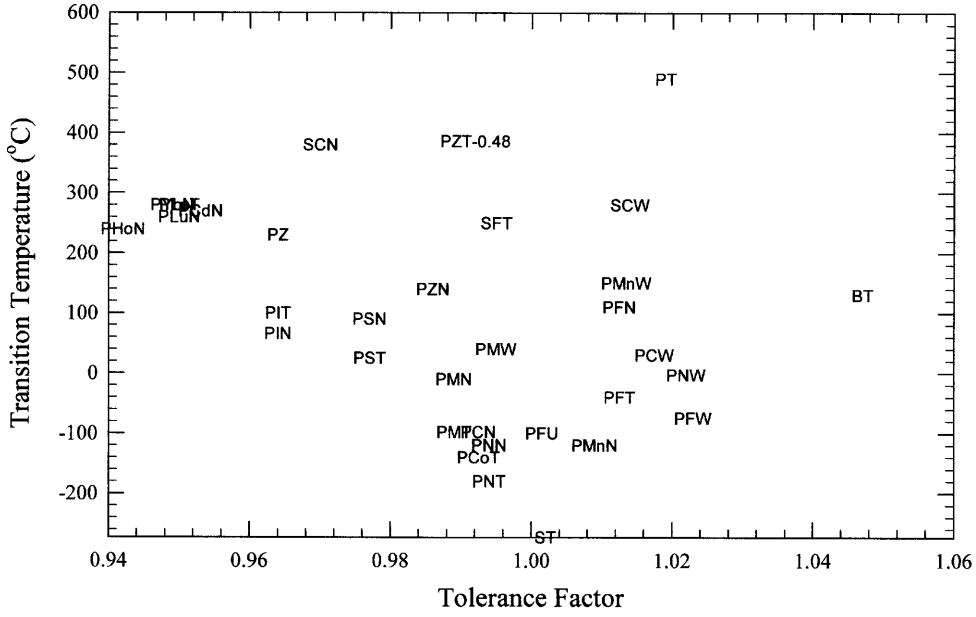

Fig. 16 T_C of MPB compositions vs. tolerance factor

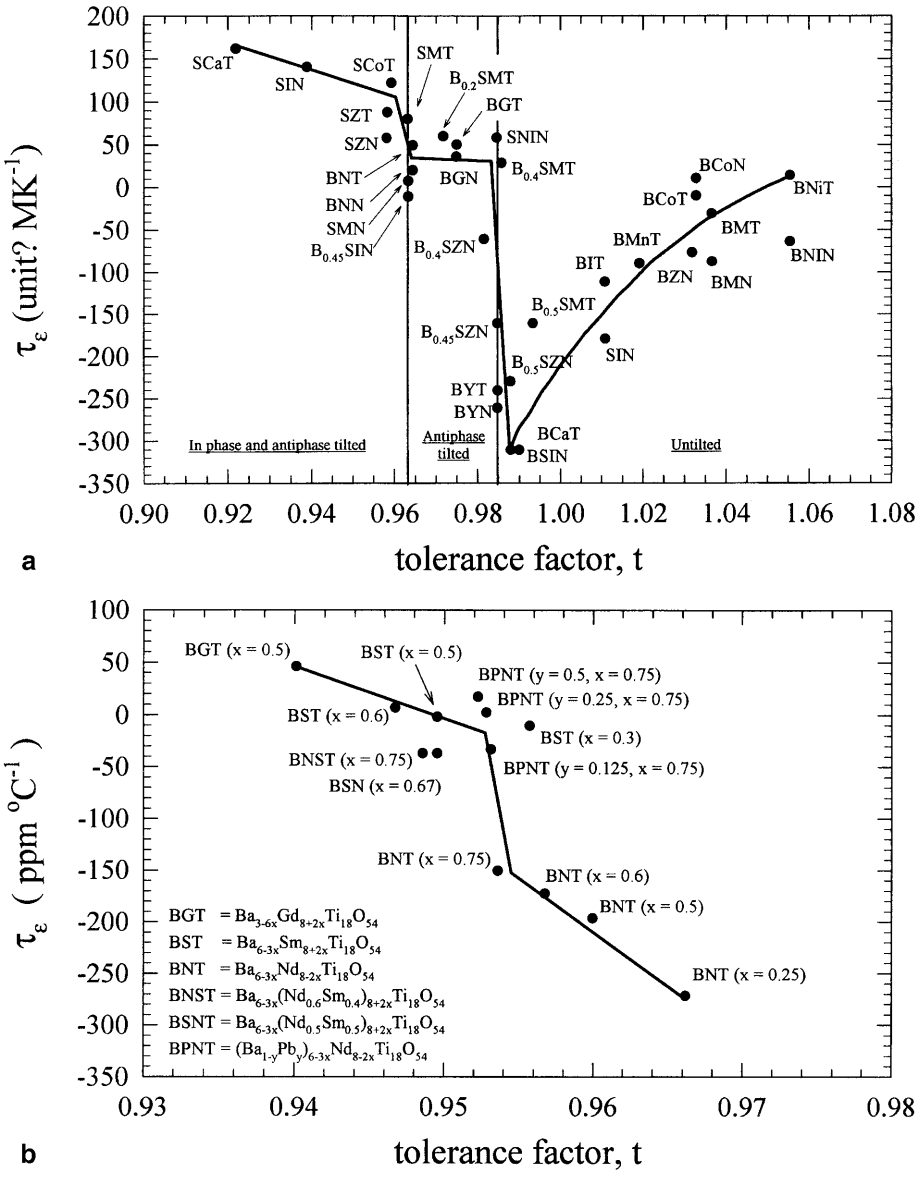

Fig. 17 (**a**) Temperature coefficients vs. tolerance factor at room temperature for some microwave dielectrics and (**b**) τ_f vs. T for BNT compounds

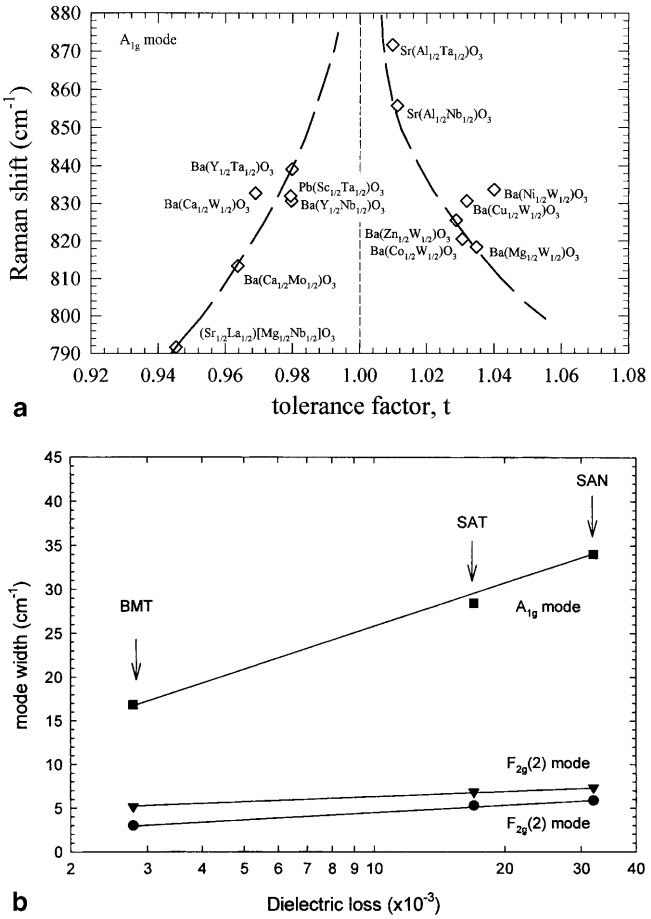

Fig. 18 (**a**) A_{1g} Raman mode shift vs. tolerance factor in perovskite structure; and (**b**) Raman mode width vs. dielectric loss in perovskites microwave dielectrics

various device-oriented properties of the perovskite structure again and again useful correlations have been found with this simple parameter. The T.F. shows how far from ideal packing the ionic sizes can move and still be "tolerated" by the perovskite structure. It reflects the structural distortion, force constants of binding, rotation and tilt of the octahedrons, etc.. These in turn affect the dielectric properties, transition temperature, temperature coefficient of the dielectric constant of material, and even the dielectric loss behavior in a perovskite dielectric.

For $t<1$, the size of the unit cell is governed by the B-site ion and as a result the A-site ions have too much room for vibration. For $t>1$, just the opposite situation occurs in the unit cell, i.e., in this case, B-site ions have too much room to vibrate. The $t=1$ condition represents the "close-packing" in the perovskite structure. It is important to mention here that all these calculations hold only when the radii of the ions used for calculating "*t*" are taken constantly from within the same tables e.g., Roy/Müller, or Shannon/Prewitt, or Goldschmidt, or Pauling. Therefore, various A- and B-site substitutions may influence properties involving restoring forces, bond strength, dipolar behavior, etc. Several properties especially related to the dielectric, phase transition behavior etc. in electronic materials correlate significantly with this simple tolerance factor approach. A few examples [74–76] (without going into details) are illustrated in Fig. 15(a), (b), and (c).

Zumuhlen et al. [74] suggested that restoring force constant of the lowest polar mode is highly influenced by the values of tolerance factors and the binding energy and consequently reflects on the magnitude of dielectric constant of a compound.

Figure 15 shows the relation of dielectric constant and transition temperature with tolerance factor in several perovskite structures. Figure 16 further expands the plots for the MPB composition materials to correlate the T_Cs of various compounds.

In Figure 17 there are plotted the temperature coefficients of a dielectric in relation to the tolerance factor.

As mentioned above, the tolerance factor may also correlate well with the peak width and frequency of a typical A_{1g} mode in Raman scattering (Fig. 18). Such features can subsequently be related back to the intrinsic dielectric losses in the perovskite family compounds in the microwave frequency region. The foregoing illustrates again the enormous value and power of the true first principles approach in science[1]: relying on the facts (empirical data) *not* the theories.

5.2 Quantum paraelectrics

Quantum paraelectric behavior is the tendency of materials to exhibit a behavior that suggests an impending phase transition at low temperatures, but the temperatures are low enough to activate quantum effects in these materials and thus the impending ferroelectric phase transition may not be realized in these cases [77]. So far the effect has been associated with only some perovskites, e.g., $SrTiO_3$ [78], $KTaO_3$, $CaTiO_3$ [79] and possibly several solid solution (RE,Na)TiO_3, where RE=La, Nd, Sm, Gd [80, 81]. When a small amount of impurities (a few ppm) are added, this class of perovskites shows a typical ferroelectric-like behavior and are thus classified as incipient ferroelectrics.

Quantum paraelectrics by virtue of their field tunability, frequency agility and low loss tangent values are promising candidates for applications in next generation communication devices. Also these materials are ideal for tunable microwave resonator and filter designs when integrated with high T_C superconductor microwave devices.

[1] Aristotle, in the Nicomachean Ethics I, vii, 20–22, clearly defines first principles in science thus: "Nor again must we in all matters alike demand an explanation of the reason why things are what they are; in some cases it is enough if the fact that they are so is satisfactorily established. This is the case with first principles; and the fact is the primary thing – it *is* a first principle. And principles are studied – some by induction, others by perception, others by some form of habituation, and also others otherwise; so we must endeavour to arrive at the principles of each kind in their natural manner, and must also be careful to define them correctly."

5.3 Unexpected application niches

5.3.1 Giant magnetoresistance (GMR)/colossal magnetoresistance (CMR)

The phenomenon is recognized as a change in resistance of a material by more than a factor of ten in the presence of magnetic field. It is interesting to note that a large number of compounds related to perovskite family $R_{1-x}A_xMnO_{3+y}$ where R refers to rare earth elements and A reefers to alkaline-earth elements (Sr, Ca, etc.) are the prime oxide compositions exhibiting giant magnetoresistance/colossal magnetoresistance effect and metal:insulator type transitions [82, 83]. Several compounds belonging to both ABO_3 and K_2NiF_4 structures exhibiting the GMR effect have been synthesized and studied in the past decade, e.g., $La_{1-x}Sr_xMnO_3$, $LaMnO_3$:Ca, (La,Pr)(Sr,Ca)MnO_3, (La,Sr)CoO_3, $LaNiO_3$, etc.

GMR oxide compounds find tremendous applications such as underwater sonar, high pressure pumps, active vibration control, damage analysis and sensors related area. There materials also have potential in high density magnetic storage technologies.

5.3.2 Catalysis

Since the 1980s perovskites have appeared in catalysis application [84, 85]. Mixed oxides of transition and rare-earth metals possessing perovskite structure appear to be suitable for such high-temperature processes as catalytic combustion, methane reforming, ammonia oxidation, sulfur dioxide reduction, etc., due to their well-known thermal stability in a broad range of oxygen partial pressures and resistance to catalytic poison [84, 85]. Recently the fact that perovskite can be both the substrate and the wash-coat, and also the active element has led to new advances by Isupova et al. [86].

Up to the present, catalytic properties of pure bulk perovskites or supported perovskites have been mainly studied and reported [86–88]. Suitable systems are rather limited but the content of the active component, and chemical interaction between active component and support at enhanced temperatures often cause loss of activity and mechanical strength. At the same time, bulk catalysts with homogeneous distribution of the structural additives and/or promoters are known to be the most thermally stable under real high-temperature conditions. Moreover, catalysts with a high content of the active component are more resistant to such catalytic poisons such as Cl, F, S-containing compounds. To minimize the pressure drop across the catalytic bed especially for gas streams with high linear velocities honeycomb monoliths are required (Fig. 19).

Pauli et al. [89, 90] developed the technology of perovskite monolith honeycomb catalyst production, the methods of preparation of highly dispersed, chemically active powders with uniform phase composition and narrow partial size distribution. Two techniques: mechano-chemical activation (MA) of solid starting compounds in high powered ball mills with a subsequent thermal treatment [89, 90] and arc plasma thermolysis (APT) of the mixed solutions of rare-earth and transition metals nitrates were both show to work [91].

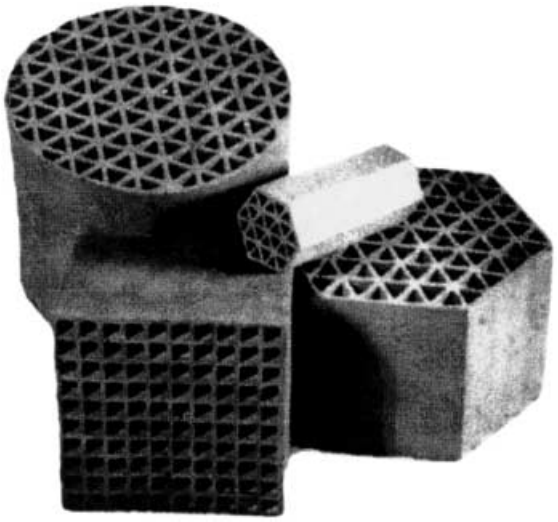

Fig. 19 Typical shapes of monolithic perovskite catalysts

5.3.3 Major materials of the Earth's mantle

Speculation as to what the inner layers of the Earth are made of are an intriguing aspect of high pressure crystal chemistry. It is now a wide belief that the major component of the lower mantle of the earth may be a perovskite-(Mg,Fe)SiO_3 [92]. Several experimental data on the conversion of ilmenite structure, $MgSiO_3$, to perovsktie at pressures ~250 kbars and temperature ~1000–1400 °C strongly supports the hypothesis. Figure 20(a) and (b) shows the ilmenite-perovskite stability range in the case of $MgSiO_3$ [52], which predominantly occurs as a substituted $(Mg_{1-x}A_x)SiO_3$ perovskite of the earth mantle. The pressure and temperature range are in the vicinity of the conditions existed at the mantle.

5.3.4 Ultrahigh melting point materials: $Ba(Mg_{1/3}Ta_{2/3})O_3$

Ceramics of the complex perovskite oxide, $Ba(Mg_{1/3}Ta_{2/3})O_3$ which crystal chemically are also analogues of PMN, have been studied extensively as potential microwave dielectrics. We have shown [73] that the BMT compound is one of the most refractory oxides so far known to science. Its refractory characteristics were not known till our attempts to grow the single crystals of BMT from its melt using the laser heated pedestal growth technique [93]. It grows congruently from the melt in the temperature range of 2900–3100 °C. A typical high temperature cubic perovskite phase was obtained at

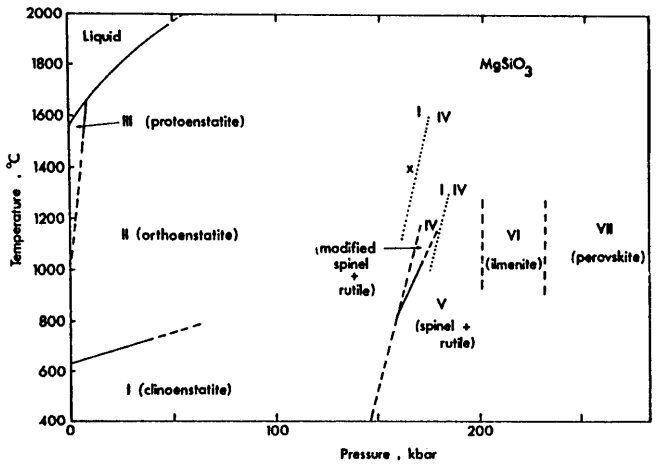

a Phase diagram of $MgSiO_3$.

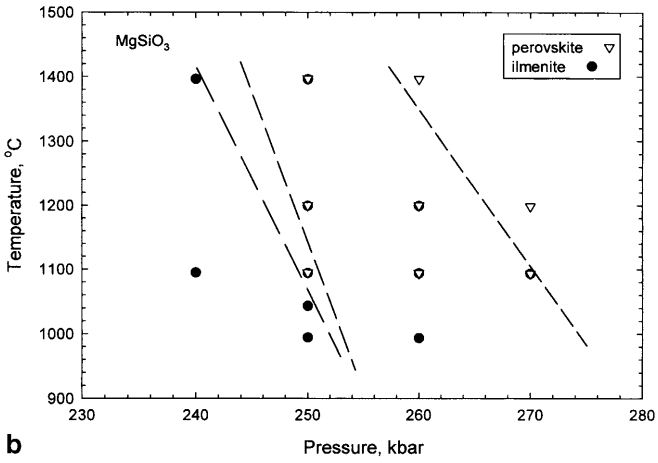

b

Fig. 20 (**a**) Phase diagram of $MgSiO_3$; (**b**) experimental data for the ilmenite-perovskite

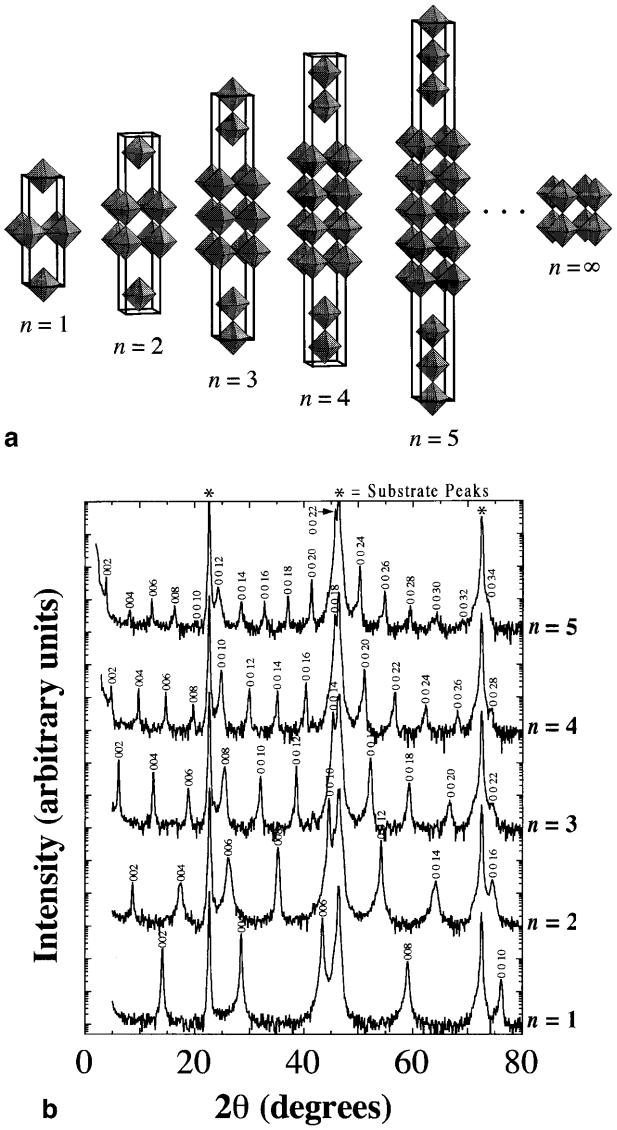

Fig. 21 $AO(ABO_3)_n$ structure – Ruddlesden and Popper phase (Schlom et al.)

room temperature, in comparison to the hexagonal, ordered perovskite ceramics usually obtained via solid state sintering. Vicker's indentation hardness test suggests the hardness of BMT single crystals are comparable to or slightly harder than Al_2O_3. These findings are highly unexpected, since the anisodesmicity caused by half-breeding of a divalent (Mg^{2+}) and pentavalent (Ta^{5+}) would have been expected to strongly *lower* the melting point.

6 Molecular engineering and design of new phases (compounds) with desired properties

It has been illustrated in earlier sections (5.1) that while simple structural descriptions such as the tolerance factor in a given perovskite compound can correlate and predict various property characteristics, such as transition temperature, temperature coefficient of dielectrics, dielectric loss, etc., it is likely that several simple crystal chemical guidelines can guide us to design the new phases/compounds with targeted electrical and mechanical properties within the perovskite family of materials. In this context we will provide a few examples which are of high technical importance and in which this approach has been exploited by us to design unique perovskites with desired properties.

6.1 Ruddlesden-popper phases and molecular engineering

The K_2NiF_4 structure in simple terms can be represented as KF layers separating the corner shared perovskite blocks. Ruddlesden and Popper [94,95] designed a series of homologous compounds with the general formula $AO(ABO_3)$ where AO represents the rock salt structure layer separating the blocks of perovskite layers characterized by n=1,2,3... ∞. Such phases exhibit properties ranging from a typical insulator or ferroelectric to a conductor or superconductor. As n increases, the phases tend to be more perovskite in nature and finally reaches the pure perovskite structure for n=∞ (Fig. 21).

Table 16 Some Ruddlesden and Popper type phases studied by various researchers (Sharma et al.)

Compound	Lattice type/symmetry
RE_2CuO_4 (RE = rare earth)	T, T′, T″, T*
$La_{n+1}Ni_nO_{3n+1}$ (*n*=1, 2, 3)	Tetragonal/monoclinic (*n*=1) Orthorhombic (*n*=2, 3)
$La_{n+1}Co_nO_{3n+1}$	Orthorhombic (*n*=1, 3) Pseudo monoclinic/tetragonal Symmetry for *n*=1 also suggested
$Sr_{n+1}Ti_nO_{3n+1}$	Tetragonal
$Sr_{n+1}Fe_nO_{3n+1}$	Tetragonal
$Sr_{n+1}Ir_nO3_{n+1}$	Tetragonal
$Sr_{n+1}Cr_nO_{3n+1}$	Tetragonal, $I4_1/acd$ (*n*=1)
$Sr_{n+1}V_nO_{3n+1}$	Tetragonal
$Sr_{n+1}Ru_nO_{3n+1}$ (*n*=1, 2)	Tetragonal
$LaSr_3Fe_3O_{10-\delta}$	Tetragonal
$Ca_{n+1}Mn_nO_{3n+1}$	$I4_1/acd$ (*n*=1)
$A_2Ln_2Ti_3O_{10}$ (A=Na, K)	Tetragonal
$Sr_3MnM'O_7$ (M′=Ru, Fe)	Tetragonal
$(A,A')_{n+1}M_nO_{3n+1}$ (*n*=1, 2, 3) (A,A′ = rare earth/alkaline earth M=Cr, Al, Ni, Fe, Mn, Ru, Ga)	Tetragonal/orthorhombic
$Ln_2Li_{0.5}Au_{0.5}O_4$	Tetragonal
La_2PdO_4	Tetragonal
Sr_2RhO_4	$I4_1/acd$
Ba_2ZrS_4/Ba_2HfS_4	I4/mmm
$Bs_4Zr_3S_{10}$	Fmmm

Recently, with the popularity of reactive MBE, it is now possible to engineer these complex phases in high structural purity. Interesting electronic properties are envisaged from such materials. Schlom et al. [96, 97] have synthesized $(SrO)(SrTiO_3)$ series and measured the targeted dielectric constant of various single crystal phases (Fig. 22). Rao et al. [98, 99] have synthesized successfully the $(LaO)(LaNiO_3)_n$ compounds. Table 16 lists some of the RP type phases studied by various workers. Such molecularly engineered materials may find applications in catalysis, electrochemistry, proton exchange and several other interesting fields [100].

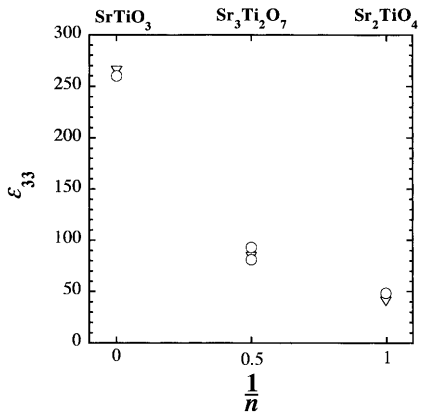

Fig. 22 Dielectric constant vs. $AO(ABO_3)_n$ structure series (Schlom et al.)

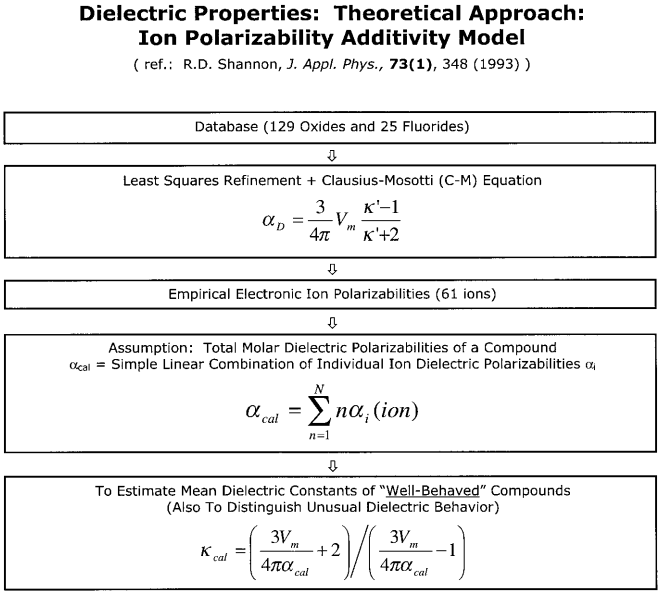

Fig. 23 Shannon's crystal chemical approach to calculate dielectric constant of materials

6.2 Shannon's approach to designing microwave dielectrics

The macroscopic dielectric constant and the polarizability of a molecule are known to be related through the Clausius-Mosotti relation:

$$\alpha_D = \frac{3}{4\pi} V_n \frac{k-1}{k+2} \tag{3}$$

where α_D is the dielectric polarizability and V_m is the molar volume in $Å^3$. While there has been no major breakthroughs in local field calculations for complex ionic solids, there has been a steadily increasing pool of experimentally measured dielectric constants of substances of various compositions and structures. An Aristotelian first principles approach will continue to dominate the high-science approach here. Dielectric polarizabilities and hence the dielectric constants of new materials and compounds whose dielectric constants have not been measured are potentially predictable by linear addition of the molecular polarizabilities of simpler substances (molecular polarizability additivity rule) [101–103] or ion polarizabilities of individual ions (ion polarizability additivity rule) [103, 104]. A review and comments about the application of polarizability additivity rules can be found in Shannon's paper [105].

Thus the κ of compositions developed by the crystal chemical approach can be calculated by the method illustrated in Fig. 23. However, in the case of complex oxide perovskites containing Ta^{5+}, Nb^{5+}, and rare earths, we have found large discrepancies between calculated and observed values. Guo et al. [106, 107] analyzed the origin of these discrepancies and expanded the Shannon model for tantalates and niobates to correctly predict the dielectric constants which agree well with the measured

Table 17 Measured and calculated dielectric constants of some tailored compositions (perovskites and complex oxides) (Guo et al.)

Substance	Symmetry	V_m	K'_{exp}	K'_{calc}	$\Delta\alpha$ (%)
$Ba(Mg_{1/3}Ta_{2/3})O_3$	Hexagonal	68.59	24.60	24.29	0.15
$(Ba_{0.8}Sr_{0.2})(Mg_{1/3}Ta_{2/3})O_3$	Cubic	67.48	25.90	21.74	2.11
$(Ba_{0.9}Sr_{0.1})(Mg_{1/3}Ta_{2/3})O_3$	Cubic	67.84	25.30	23.48	0.88
$CaNdAlO_4$	Tetragonal	82.30	19.65, 17.65	18.34	–0.29
$CaYAlO_4$	Tetragonal	78.88	21.44, 16.12	22.44	1.97
$LaAlO_3$	Rhombohedral	54.40	21.90	22.39	–0.87
$Nd_{0.39}Sr_{0.61}Al_{0.695}Ta_{0.305}O_3$	56.76	24.04	22.17	1.01	
$PrAlO_3$	Rhombohderal	53.25	25.00	25.99	0.44
$Sr(Al_{0.5}Ta_{0.5})O_3$ ordered	Cubic	59.09	11.78	17.10	–7.76
$Sr(Al_{0.5}Ta_{0.5})O_3 - 0.3\ LaAlO_3$	Cubic	58.08	21.90	22.75	–0.50
$Sr(Al_{0.5}Ta_{0.5})O_3 - 0.3\ NdGaO_3$	Cubic	57.90	16.30	21.89	–4.59
$SrLaAlO_4$	Tetragonal	89.15	16.81, 20.02	18.77	0.61

values. Table 17 lists (along with some other complex oxides) some examples of tailored perovskite compositions and their measured and predicted (calculated) dielectric constants. The agreement in values is remarkable.

In addition, if the compositions are designed with the appropriate tolerance factor value, then engineered materials will also exhibit the low loss in the microwave frequency range.

7 Summary

The history of the utilization of perovskite-structured phases is an object lesson in the value of crystal chemistry. It is quite clear from the examples given or referred to in this article that the perovskite structure is an extraordinarily versatile one. It provides an essential family of materials for a wide variety of present day technologies and is likely to be an integral part of the future developments needed in high frequency communication and several other integrated technologies. The diversity of perovskite structure compounds which can be synthesized, provides the extreme range of electrical, magnetic, optical and mechanical properties over a wide temperature range. This could be a special boon to the integrated technologies where compatibility of the structure of various materials, with different functional properties is a major concern, since the structural mismatch often leads to various ageing, failure and impractical operating limitations for devices. By using the vast crystal chemistry resources and principles (e.g., ionic radii, valence, tolerance factor, etc.) innumerable perovskite compounds with variety of properties can be designed and yet provide the structural identity to facilitate superior integrated devices. As mentioned in this article, several highly technologically important properties from macro to nanoscale have already been identified in this class of materials. Perovskite structure compounds, no doubt, are and will be an integral part of the important commercial and strategic/special technologies of the future. As we step into the future nanoscale technologies such as high density packaging, low and ultra-low temperature and HTSC based electronics, spintronics, high Q and compact microwave components etc., the unique perovskite structure has the potential to provide a wealth of new compounds with unique properties. With the availability of new nanoscale deposition and fabrication tools for material preparation, a perovsktie material can be engineered which can exhibit more than one desirable property for new device concepts.

Acknowledgements We are thankful to many of our colleagues and students for invaluable contributions in various aspects of the related research. Financial support from federal, state, and industry for various projects throughout the years were also instrumental for some of the findings.

References

1. Muller O, Roy R (1974) The Major Ternary Structural Families, Springer, Berlin Heidelberg New York
2. Swanson HE et al. (1953–1960) NBS Circ 549, vol 1–10
3. Perowskite R (1839) Ann Phy 48:558; 2:128
4. Perowskite R (1877) Dysanalyte Knop Zs Kr 1:284
5. Goldschmidt VM (1927) Geochemisce Verterlungsgesetze der Elemente. Norske Videnskap, Oslo
6. Pauling L (1960) Nature of the Chemical Bond, Bornell University Press, Ithaca NY
7. Wainer E, Soloman S (1942) Titanium Alloy Manufacturing Co. Report 8–9
8. Wul BM, Goldman IM (1945) Doki Akad. Nauk SSSR 46:154
9. Ogawa, see in Miyake S, Ueda R (1946) J Phys Soc Jpn 1:32
10. Newnham RE, Cross LE (1990) In Kyoui no Chitabari (on $BaTiO_3$) p 325, published by Murata Co, Japan
11. Sheldrake R, Bohm D (1982) "Morphogenetic fields and the implicate order," ReVision 5:41
12. von Hippel A (1959) Molecular Science and Molecular Engineering, MIT Press, Cambridge, MA
13. Ginsberg VL (1945) J Expt Theor Phys SSR 15:739 (in Russian)
14. Megaw H (1945) Nature (London) 155:484
15. Blattner H, Matthias B, Merz W (1947) Helv Phys Acta 20:225
16. Matthias B, von Hippel A (1948) Phys Rev 73:1378
17. Cross LE, Dennison AT, Nicholson M (1949) Proc Leeds, Phil Soc 5:199
18. Blattner H, Kaenzig W, Merz W (1949) Helv Phys. Acta 22:35
19. Devonshire AF (1949) Phil Mag 40:1040
20. Kay HF, Vousden P (1949) Phil Mag 40:1019
21. Roy R (1956) J Am Ceram Soc 49:145
22. DeVries RC, Roy R (1955) J Am Ceram Soc 38:142
23. DeVries RC, Roy R, Osborn EF (1955) J Am Ceram Soc 38:158

24. Rase DE, Roy R (1955) J Am Ceram Soc 38:389
25. Roy R, Osborn EF (1954) Am Mineralogist 39:853
26. Komarneni S, Roy R, Breval E, Ollinen M, Suwa Y (1986) Advanced Ceramic Materials 1:87
27. Roy R (1996) Fifty-Year Perspective on Hydrothermal Research. In Proceedings 1st Intl Workshop on Solvothermal and Hydrothermal Reactions. Takamatsu, Japan, p 1
28. Ravichandran D, Meyer R Jr, Roy R, Guo R, Bhalla AS, Cross LE (1996) Materials Research Bulletin 31:817
29. Ravichandran D, Yamakawa K, Bhalla AS, Roy R (1997) J Sol-gel Science and Technology 9:95
30. Yamakawa K, Ravichandran D, Trolier-McKinstry S, Dougherty JP, Roy R, Bhalla AS (1997) Ferroelec Lett 22:41
31. Roy R, Tuttle OF (1956) Investigations Under Hydrothermal Conditions. In Physics and Chemistry of the Earth 1:138–180, Pergamon Press
32. DeVries RC, Roy R (1958) Econ Geol. 59:958
33. Moon J, Li T, Randall C, Adair JH (1997) J Mat Res 12:189
34. Kutty TRN, Balachandran R (1984) Mat Res Bull 19:1479
35. Phule PP et al (1990) Ceram Transact 12:725
36. Hawkins DB, Roy R (1963) Geochim Cosmochim Acta 27:1047
37. Yoshimura M, Yoo S-E, Hayashi M, Ishizawa M (1989) Jpn J Appl Phys 28:L2007
38. Cheng JP, Agrawal DK, Komarneni S, Mathis M, Roy R (1997) Mater Res Innov 1:44
39. Bhalla AS, Nair KM (eds) (1992) Ferroelectric Films. Ceramic Transactions. Am Ceram Soc, Westerville, OH
40. "Modeling and simulation of thin-film processing", Materials Research Society Symposia Proceedings, V. 389, Pittsburgh, PA, Materials Research Society (1995)
41. Journal of Integrated Ferroelectrics, Gordon and Breach Publication (1981–)
42. Roy R (1954) J Am Ceram Soc 37:581
43. Keith ML, Roy R (1954) Am Mineralogist 39:1
44. Galasso F (1970) Structure and Properties of Inorganic Solids. Pergman Press, Oxford, New York
45. Stability of Metallic Structures (1967) In: Phase Stability in Metals and Alloys. McGraw-Hill, New York, chap 3
46. Zunger A, Engelsi N (1964) ASM Transac 57:610
47. Phillips JC (1970) Physics Today 23:23
48. Phillips JC (1969) Phys Rev Letters 22:649
49. Muller O, White WB, Roy R (1964) J Inorg Nuc Chem 26:2075
50. Sleight WA (1968) Inorg Chem 7:1704
51. Rase DE, Roy R (1955) J Am Ceram. Soc 38:102
52. See Phase Diagrams for Ceramists: bibliographic update through January 1, 1989 and cumulative indexes for volumes I-VIII," American Ceramic Society (1990)
53. Newnham RE, Cross LE (1974) Mat Res Bull 9:92
54. Lines ME, Glass AM (1977) Principles and Applications of Ferroelectrics and Related Materials. Oxford University Press, London
55. Smolenski GA, Isupov VA, Agranovskaya AI (1959) Sov Phys Sol State 1:909
56. Cross LE (1987) Ferroelectrics 76:241
57. Bhalla AS (1993) Presented at ONR Workshop, University of Maryland
58. Randall CA, Bhalla AS (1990) Jpn J Appl Phys 29:327
59. Jaffe B, Cook WR Jr, Jaffe H (1971) Piezoelectric Ceramics. Academic Press, London and New York
60. Alberta E, Guo R, Bhalla AS (2000) Ferroelectrics Rev 3 (to be published)
61. Guo R, Bhalla AS, Roy R, Cross LE (1994) Epitaxial Oxide Thin Films and Heterostructures 341:215. MRS Publications
62. Newnham RE, Skinner DP, Cross LE (1978) Mat Res Bull 13:525
63. Roy R (1996) Widespread Occurrence of the Nano Composite State and Principles for Its Exploitations. In Frontier Nanostructured Ceramics. Tohwa Univ. Press, Fukuoka, Japan. p 3
64. Freer R (1993) Silicates Industries 9:191
65. Ganguly P, Rao CNR (a) Mat Res Bull 8:408 (1973); (b) J Sol State Chem 24:820 (1979)
66. Sleight AW, Gilson JL, Bierstedt PE (1975) Sol State Commun 17:27
67. Gilbert LR (1980) PhD Thesis, The Pennsylvania State University
68. Gilbert LR, Messier R, Roy R (1978) Thin Solid Films 54:129
69. Bednorz JG, Muller KA (1986) Z Phys B64:189
70. See Bhalla AS, Roy R, Cross LE (1988) In Chemistry of Oxide Superconductors. Blackwell Scientific Publications. p 71
71. Ashburn JR (private communication)
72. Wu MK, Ashburn JR, et al (1987) Phys Rev Lett 58:908
73. Bhalla A, Guo R (1997) Acta Physica Polonica A 92:7
74. Zumuhlen R, et al (1995) J Appl Phys 77:5341; 77:5351
75. Katiyar R, Siny IG, Guo R, Bhalla AS (1990) Materials Transac 511:165
76. Siny IG, Katiyar R, Bhalla A (to be published) J Phys Chem Sol
77. Weaver HE (1959) J Phys Chem Solids 11:274
78. Möller KA, Burkhard H (1979) Phys Rev B19:3593
79. Bhalla AS, Jiang Y, Guo R, Ferroelect Lett (to be published).
80. Venkateshwaran B, Guo R, Bhalla AS (1999) J Inorg Matls 1:395
81. Bhalla A (1999) Presentation at the Am Ceram Soc Meeting. Cincinnati, OH
82. Rao CNR et al (a) J Sol State Chem 22:353 (1977); (b) Science 272:369 (1996)
83. Von Helmos R et al (1993) Phys Rev Lett 71:2332
84. Trimm DL (1983) Appl Catal 7:249
85. Tejuca LG, Fierro JLG, Tascon JMD (1989) Adv Catal 36:237
86. Isupova LA, Sadykov VA, Tikhov SF, Kimkhai ON, Kovalenko ON, Kustova GN, Ovsyannikova IA, Dovbii ZA, Kryukova GN, Rozovskii AY, Tretyakov VF, Lumin VV (1994) React Kinet Catal Lett 53:223
87. Baran ET (1990) Catalysis Today 8:133
88. Yamaxoe V, Tekaoka J (1990) Catalysis Today 8:175
89. Pauli IA, Avvakumov EG, Isupova LA, Poluboyarov VA, Sadykov VA (1992) Sib Khim Zhurn 3:133 (Russian)
90. Isupova LA, Sadykov VA, Solovyova LP, Andrianova MP, Ivanov VP, Kryukova GN, Kolomiichuk VN, Avvakumov E, Pauli IS, Andryushkova OV, Poluboyarov VA, Rozovskii AY, Tretyakov VF (1994) Proc 6th Intl Symp Scientific Bases for the Preparation of Heterogeneous Catalysts 2:231. Louvain-la-Neuve. 5–8 Sept
91. Tikhov SF, Sadykov VA, Pack EA, Kimkhai ON, Moroz EM, Ivanov VP, Kustova GN, Alikina GM (1991) Proc 7th Intl Symp Heterogeneous Catalysis 2:423. Bourgas
92. Tschauner O, Zerr A, et al (1999) Nature. April 15
93. Guo R, Bhalla AS, Cross LE (1994) J Appl Phys 75:4704
94. Ruddlesden SN, Popper P (1957) Acta Cryst 10:538
95. Ruddlesden SN, Popper P (1958) Acta Cryst 11:54
96. Schlom D, Theis CD, Hawley ME (1998) Ceram Transac 86:41
97. Haeni JH, Theis CD, Schlom D (to be published) Appl Phys Lett
98. Rao CNR (1985) Bull Mat Sci 1:155
99. Rao, CNR, Thomas JM (1985) Acc Chem Res 18:113
100. Sharma JB, Singh D (1998) Bull Mat Sci 21:363 (and references therein)
101. Heydweille AR (1920) Z Phys 3:308
102. Narayana Rao DAAS (1949) Proc Ind Acad Sci 30A:317
103. Langa AC, Cygan RT (1942) Am Mineral 67:328
104. Roberts R (1949) Phys Rev 76:1215
105. Shannon RD (1993) J Appl Phys 73:348
106. Guo R, Bhalla AS, Roy R, Cross LE (1994) Ferroelectrics 155:43
107. Guo R, Bhalla AS (1998) Ceramic Transactions 84:139